R-07-61

SFR inverse modelling Part 2

Uncertainty factors of predicted flow in deposition tunnels and uncertainty in distribution of flow paths from deposition tunnels

Johan Holmén, Golder Associates

October 2007

Svensk Kärnbränslehantering AB
Swedish Nuclear Fuel
and Waste Management Co
Box 5864
SE-102 40 Stockholm Sweden
Tel 08-459 84 00
+46 8 459 84 00
Fax 08-661 57 19
+46 8 661 57 19

ISSN 1402-3091
SKB Rapport R-07-61

SFR inverse modelling Part 2

Uncertainty factors of predicted flow in deposition tunnels and uncertainty in distribution of flow paths from deposition tunnels

Johan Holmén, Golder Associates

October 2007

Keywords: dokID 1089789, SFR 1 SAR-08, Hydrogeology, Inverse modelling.

Preface

This document describes the uncertainty in the tunnel flow and distributions of flow paths from the storage tunnels. The study is a continuation of the hydrogeological modelling performed within the SAFE project. This document constitutes one of the references describing the hydrogeology at SFR and is used in the safety analysis SFR 1 SAR-08.

Johan Holmén, Golder Associates has compiled the report.

This document has been reviewed and all comments have been documented in accordance with SKIFS 2004:1.

Stockholm, November 2007

Anna Gordon
Project leader, SFR 1 SAR-08

Contents

1 Introduction and purpose

1.1 Background

The Swedish Nuclear Fuel and Waste Management Co (SKB) is operating the SFR repository for low- and intermediate-level nuclear waste. An update of the safety analysis of SFR was carried out by SKB as the SAFE project (Safety Assessment of Final Disposal of Operational Radioactive Waste). The aim of the project was to update the safety analysis and to produce a safety report. The safety report has been submitted to the Swedish authorities.

This study is a continuation of the SAFE project, and concerns the hydrogeological modelling of the SFR repository, which was carried out as part of the SAFE project, by /Holmén and Stigsson 2001ab/.

The Swedish authorities, SKI and SSI, has examined the SAFE project. Their findings are presented in an examination report: /SKI 2003:37/ (also printed as /SSI 2003:21/). The results of the examination of the hydrogeological modelling by /Holmén and Stigsson 2001ab/ are presented in the report of the Swedish authorities. We may conclude the review of the hydrogeological model in the following way: The modelling presented in /Holmén and Stigsson 2001ab/ would be improved if an attempt was made to quantify the uncertainty of the calibration of the hydrogeological model.

The uncertainty in the calibration of the hydrogeological model of SFR-1 /Holmén and Stigsson 2001ab/, was analysed in /Holmén 2005/ by use of an inverse modelling procedure. The uncertainties of the calibration were propagated into predictive simulations and the influence of the calibration uncertainties on the values of tunnel flow, as given in /Holmén and Stigsson 2001ab/, were thereby estimated, and the results are presented in /Holmén 2005/.

The inverse modelling procedure of /Holmén 2005/ were based on the same general conceptual model as was used in /Holmén and Stigsson 2001ab/; therefore the uncertainties analysed in /Holmén 2005/ were linked to the conceptual model of /Holmén and Stigsson 2001ab/.

The evaluated uncertainties were limited to the following parameters:

- Uncertainty in conductivity of rock mass between local and regional fracture zones.
- Uncertainty in transmissivity of local and regional fracture zones. The model includes 6 different fracture zones: Singö zone, Zone H2, Zone 3, Zone 6, Zone 8 and Zone 9.
- Uncertainty in properties of a hydraulic skin that surrounds the tunnels of the SFR. The skin will reduce the groundwater inflow to the tunnels when the tunnels are drained. The skin will however not reduce the future flows through the tunnels when the tunnels are resaturated.
- Uncertainty in measured inflow of groundwater to the tunnel system.
- Uncertainty in amount of inflowing groundwater that is evacuated via air ventilation.
- Uncertainty considering an internal heterogeneity of the permeability of the rock mass between identified fracture zones.
- Uncertainty caused by the combination of the parameters discussed above.

At a meeting at SKB (12/10 2006) plans were presented by SKB for renewed calculations of the future transport of nuclides from the deposition tunnels at SFR. These new calculations should include the estimated calibration uncertainties as presented in /Holmén 2005/.

In addition to the variation of flow in the tunnels, as presented in /Holmén 2005/, the renewed transport calculations also need an estimate of the uncertainty in the distributions of flow paths from the deposition tunnels.

This short report will not include a detailed presentation of the system of tunnels at SFR or a presentation of the hydrogeology in the surroundings of the SFR, nor a presentation of the models utilized for estimation of the future groundwater flows at SFR. For such descriptions we refer to the /Holmén and Stigsson 2001ab/ and the /Holmén 2005/ studies.

The tunnel system is however presented briefly in Figure 1-1. The topography of the area studied and the position of the tunnel system as well as the estimated retreat of the shoreline is presented in Figure 1-2, below. In addition a brief visualization of the tunnels and fracture zones is presented in Appendix A.

1.2 Purpose of study

This study has two purposes: (i) presentation of uncertainty factors and (ii) calculation and analyses of flow paths. The study also includes a brief discussion of the hydraulic importance of tunnel plugs.

Uncertainty factors

The statistical distribution of predicted future flows in the tunnels of SFR is the final results of the /Holmén 2005/ study. The range of flow values are given as probability distributions. In addition to these distributions of predicted flows, the /Holmén 2005/ study also includes the concept of uncertainty factors. The uncertainty factors relate the results of the inverse modelling procedure of /Holmén 2005/ to the results presented in /Holmén and Stigsson 2001ab/. The methodology of the uncertainty factors are discussed in Section 2.1. It is a purpose of this study to present individual uncertainty factors for the different deposition tunnels, considering the base case of /Holmén 2005/ and the 60 accepted realizations of the base case of /Holmén 2005/. Two different flow situations will be studied. (i) The flow situation at time equal to 2,000 AD, this situation represents a closed and resaturated repository with the sea at its present level. (ii) The flow situation at time equal to 4,000 AD, this situation represents a closed and resaturated repository with the sea at an estimated future lower level, caused by the shore line displacement /see Holmén and Stigsson 2001ab/. The flow in the tunnels will not change after approximately 4,000 AD. Therefore the 4,000 AD situation may be used as a representation of future steady state similar situations when considering the flow in the deposition tunnels.

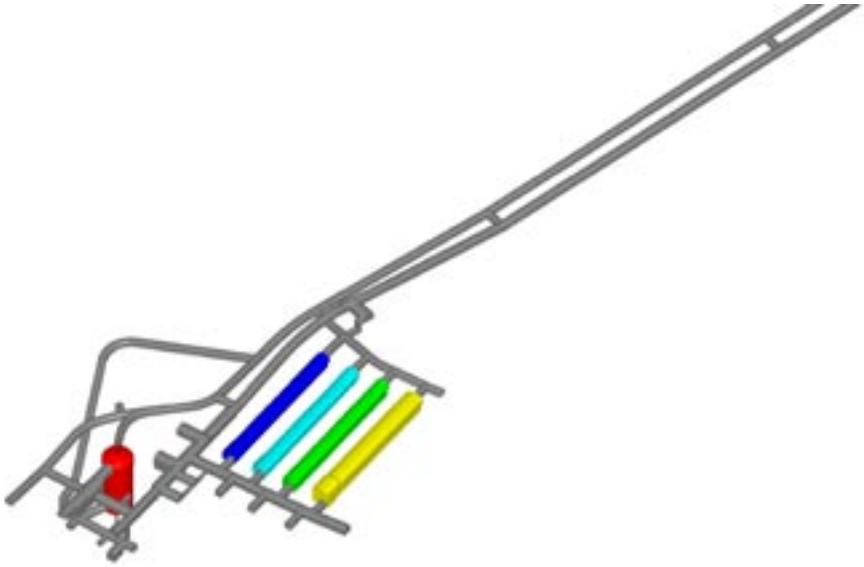

Figure 1-1. *The general layout of the tunnel system at SFR. The grey colour denotes the access tunnels. The red colour denotes the SILO. The dark blue colour denotes the BTF1 and the light blue denotes the BTF2. The green colour denotes the BLA tunnel. The yellow colour denotes the BMA tunnel.*

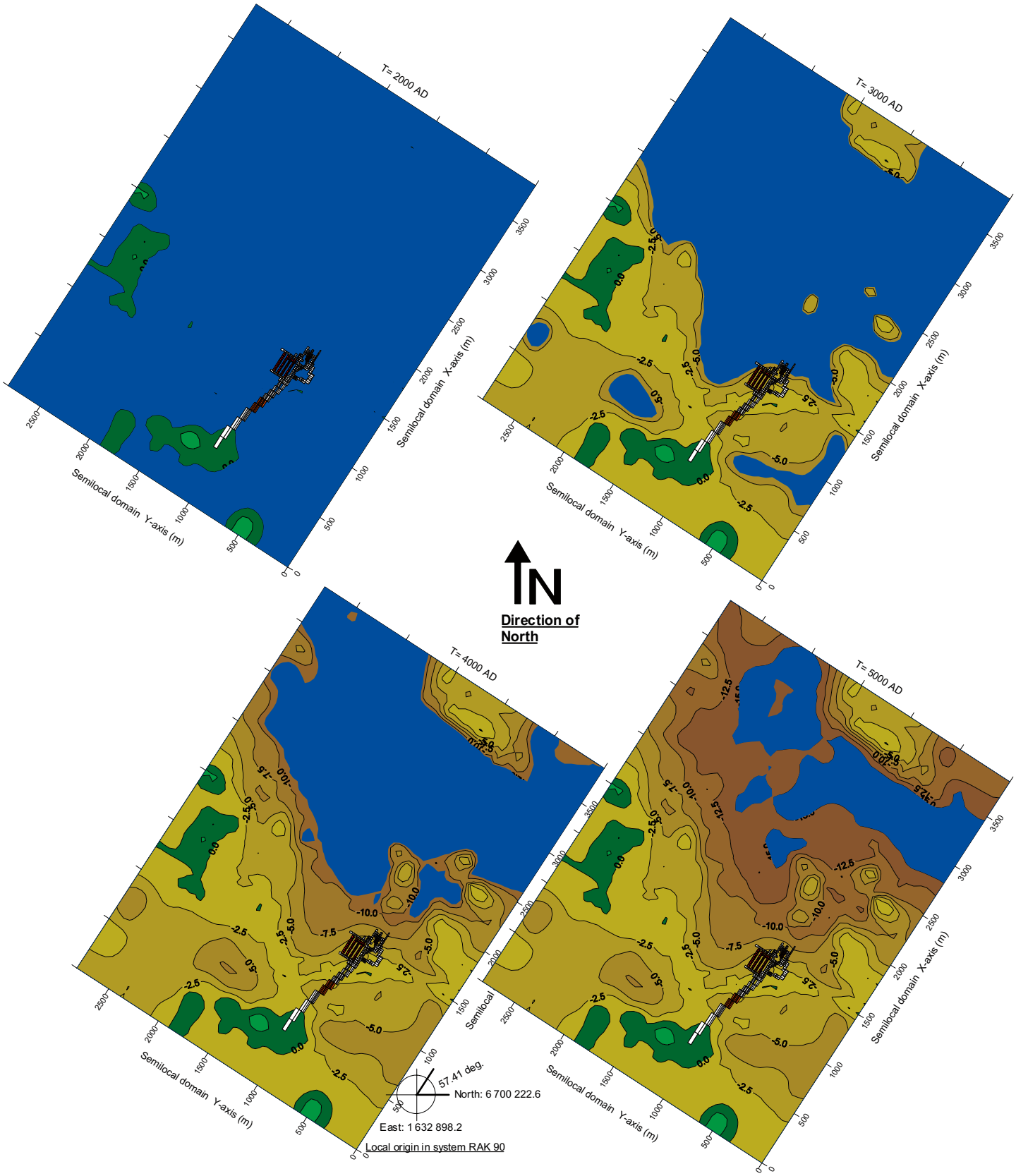

Figure 1-2. *Semilocal domain, the topography, the retreat of the shoreline and the position of the SFR repository. The figure depicts the following times: upper left is 2,000 AD, upper right is 3,000 AD, lower left is 4,000 AD and lower right is 5,000 AD. The horizontal position of the tunnel system at SFR is also marked in the figures.*

Flow paths

Flow paths from the deposition tunnels will be generated and analysed, considering the base case of /Holmén 2005/ and the 60 accepted realisation of the base case of /Holmén 2005/. Two different flow situations will be studied. (i) The flow situation at time equal to 2,000 AD, this situation represents a closed and resaturated repository with the sea at its present level. (ii) The flow situation at time equal to 5,000 AD, this situation represents a closed and resaturated repository with the sea at an estimated future lower level, caused by the shore line displacement /see Holmén and Stigsson 2001ab/. The distribution of flow paths from the deposition tunnels will not change after approximately 5,000 AD. Therefore the 5,000 AD situation may be used as a representation of future steady state similar situation when considering flow paths from the deposition tunnels. The groundwater flow situation at 4,000 AD is studied when the different flows of the deposition tunnels are estimated, but the flow situation at 5,000 AD is studied when the distributions of flow paths are estimated. This is because the discharge points of the flow paths have a tendency to follow the retreating shoreline, even after the time when flows of the tunnels have reached a steady state similar situation. At 4,000 AD the shore line is at a certain distance form the tunnels, but the shoreline is still retreating. At 5,000 AD, a local lake has been created east of the SFR repository and the water level of this lake is steady (in the model). At 5,000 AD the retreat of the shoreline is no longer influencing the flow paths from the deposition tunnels, since the water level of the lake is not changing and as the shoreline is far away form the SFR. The reader may perhaps be worried that the flow paths from 5,000 AD will not match the flows from 4,000 AD, such a worry is however unfounded as the tunnel flows are the same at 4,000 AD and at 5,000 AD (for the established model).

1.3 Applicability of established models

The established models are based on the calibrated model of /Holmén and Stigsson 2001ab/ as well as on the inverse modelling of /Holmén 2005/. The models of /Holmén and Stigsson 2001ab/ and /Holmén 2005/ are based on all available and applicable data of the system studied, including a detailed description of the tunnel system.

The models of /Holmén and Stigsson 2001ab/ and /Holmén 2005/ reproduces the measured inflow of groundwater to the tunnel system of SFR. In addition the inverse modelling of /Holmén 2005/ estimates the uncertainty of the hydraulic properties of the rock masses and fracture zones that surrounds the tunnels based on the measured inflow of groundwater to the tunnels; and the inverse modelling includes uncertainty in measurements of the inflow, and also the importance of a hydraulic skin that may surround the tunnels of SFR. (A hydraulic skin will reduce the inflow to the tunnels when the tunnels are drained, but will not reduce the flow though the tunnels when the tunnels are no longer drained.)

The inverse modelling of /Holmén 2005/ does not only estimate the uncertainty of the calibration of the flow model of /Holmén and Stigsson 2001a/, but the /Holmén 2005/ study also estimates the corresponding importance of the uncertainty of the calibration when simulating (predicting) the future flows of the studied system.

The importance of the uncertainty of the calibration when simulating the future flows of the studied system is given by the 60 accepted realizations of /Holmén 2005/, when these realizations are used for modelling of future flow situations.

The modelling presented in this study is based on the 60 accepted realizations of the base case of /Holmén 2005/, therefore this modelling includes the estimated uncertainty of the properties of the rock mass and of the fracture zones, estimated uncertainty in measured inflow to tunnels and estimated uncertainty in hydraulic skin, when simulating a future flow situations at SFR. The established models are applicable considering the purpose of the study.

2 Uncertainty factors

2.1 Methodology

The statistical distribution of predicted future flows in the tunnels of SFR is the final result of the /Holmén 2005/ study. The range of flow values are given as probability distributions. In addition to these distributions of predicted flows, the /Holmén 2005/ study also includes the concept of uncertainty factors.

The uncertainty factors are calculated by relating the results of the /Holmén 2005/ study (predicted flows) to the corresponding flow values in /Holmén and Stigsson 2001ab/. The resulting uncertainty factors may be used in combination with the detailed results given in /Holmén and Stigsson 2001ab/. By multiplying the detailed results given in /Holmén and Stigsson 2001ab/ with an uncertainty factor, it is possible to derive a value of flow from /Holmén and Stigsson 2001ab/ that corresponds to a certain uncertainty or accepted realisation of the /Holmén 2005/ study.

For example, the flow in a certain part of a tunnel, at a certain time, and for a certain realisation is estimated by multiplying the flow value given in /Holmén and Stigsson 2001ab/ by the uncertainty factor of /Holmén 2005/ that corresponds to the tunnel studied, the time studied and the realisation studied.

The uncertainty factor (U) is calculated as:

$u = Q_{NEW} / Q_{OLD}$

Q_{NEW} = Predicted flow of /Holmén 2005/
Q_{OLD} = Calibrated flow of /Holmén and Stigsson 2001a/

Uncertainty factors (u-factors) have been calculated for each deposition tunnel and for each accepted realization of the properties of the rock mass that surrounds the SFR. (An accepted realization is a realization that has passed all tests of the inverse modelling procedure of the /Holmén 2005/ study.)

By applying a statistical analysis of the distribution of u-factors it is possible to calculate u-factors that correspond to certain probabilities, e.g. an uncertainty factor that corresponds to the 90th percentile of flow values. This is the way the u-factors are presented in /Holmén 2005/.

Hence, in /Holmén 2005/ the distribution of the uncertainty factors (taken over multiple realizations) was presented, in this study we will use the individual realizations for analyses of correlations, and calculations of flow paths etc, the individual realizations may be looked upon as samples from the ensemble of accepted realizations.

2.2 Correlation of uncertainty factors within an accepted realization

Since u-factors are calculated for each deposition tunnel there will be five u-factors for each accepted realisation, corresponding to the BMA, BLA, BTF1, BTF2 and SILO deposition tunnels. It was argued at the meeting at SKB (06-10-12) that perhaps it is not necessary to propagate all u-factors of all realisations to the transport modelling. If there is a strong positive correlation between the u-factors within a realisation it should perhaps be possible to set up a more simplified approach in the transport modelling. An example: There is a strong positive correlation if the u-factor that represents the BMA tunnel is large and for the same realisation the u-factors of the SILO and the other tunnels are large as well.

The correlation has been investigated by scatter plots representing a future flow situation with the sea at the 2,000 AD level. The plots relate the u-factors of different tunnels. If there is a strong positive correlation, the dots of the scatter plots should create narrow bands in the figures, directed from the lower left corner towards the upper right corner. If the correlation is weak the dots of the scatter plots will form bands with large widths. If the dots form semi-circular clouds there is no correlation. The results for two typical situations are given below in Figure 2-1 and in Figure 2-2.

Figure 2-1 presents the correlation between the u-factors of the BLA tunnel and the BMA tunnel, considering a flow situation with the sea at the 2,000 AD level. Each dot in the figure represents an accepted realization. From the figure it can be concluded that there is a positive correlation, but the correlation is far from perfect. Approximately the same correlation can be seen when the u-factors of the BMA, BLA, BTF1 and BTF2 tunnels are compared. The positive correlations and the similar looking correlations of the BMA, BLA and BTF tunnels follow probably from the properties of fracture zone 6 which intersects these tunnels.

Figure 2-2 presents the correlation between the u-factors of the SILO tunnel and the BMA tunnel, considering a flow situation with the sea at the 2,000 AD level. Each dot in the figure represents an accepted realization. From the figure it can be concluded that there is no positive correlation between the u-factors of the BMA tunnel and the u-factors of the SILO tunnel. Hence, it is fully possible that the u-factor of the SILO is large and for the same realization the u-factor for the BMA is small. This is also a consequence of fracture zones that intersects the tunnels of SFR; Zone 6 is very important for the flow of the BMA tunnel, but Zone 6 is of minimal importance for the flow of the SILO.

Based on the results presented in Figure 2-1 and Figure 2-2 we conclude the following: There is a positive correlation of the u-factors within the accepted realization when considering the BMA, BLA and BTF tunnels. This is the reason why it is necessary to propagate each individual u-factor to the transport modelling, together with the other corresponding u-factors for each

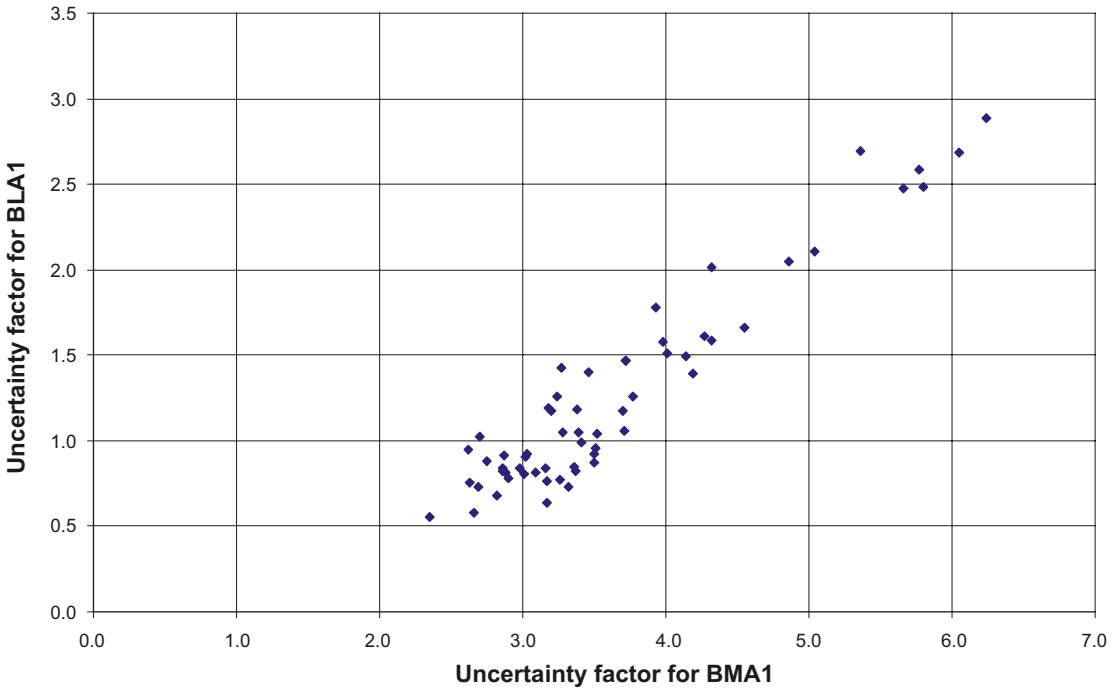

Figure 2-1. *Correlation between uncertainty factors of the BLA and the BMA deposition tunnels. Each dot represents an accepted realization. Flow situation 2,000 AD. Base case.*

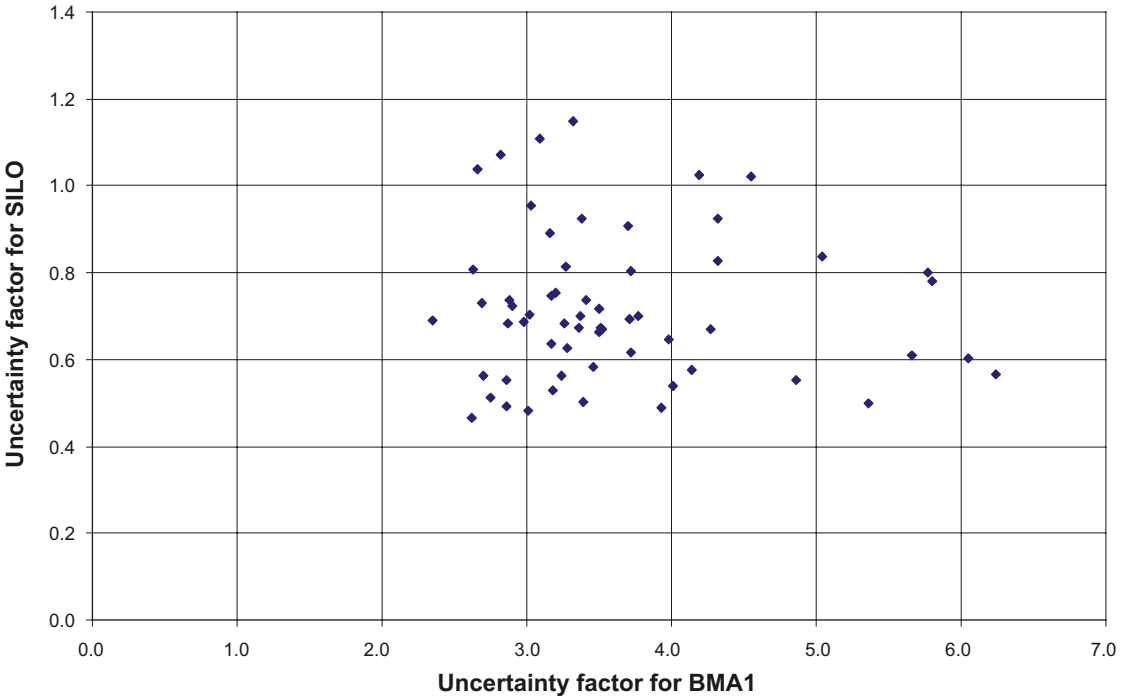

Figure 2-2. *Correlation between uncertainty factors of the SILO and the BMA deposition tunnels. Each dot represents an accepted realization. Flow situation 2,000 AD. Base case.*

realization studied. If the u-factors are treated as independent in the transport modelling, it may happen that in the transport modelling the u-factor for e.g. the BMA is large and the u-factor for the e.g. the BLA is small, this is however not correct, as the correlation analysis demonstrates that if the flow is large in one of the four tunnels BMA, BLA, BTF1 and BTF2 it is likely that the flow is large in the other three tunnels as well. The u-factor of the SILO is more or less independent of the u-factors of the other deposition tunnels (note for example row 10 in the matrix given below in Table 2-1). Hence, it is necessary to propagate each individual u-factor to the transport modelling; a simplified approach is not recommended.

2.3 An example of a matrix of uncertainty factors and a discussion of how to implement them in a transport model

A good approach is to propagate a matrix of u-factors from the SFR inverse flow modelling /Holmén 2005/ to the new transport modelling. Each row in the matrix represents an accepted realisation and each column of the matrix represents a deposition tunnel.

The transport modelling should be carried out based on a stochastic approach which includes a large number of different realizations. When the groundwater flows of the deposition tunnels are specified for a certain realization of the transport model, a single row of u-factors should be randomly selected from the matrix (same probability for all rows). The flow of different parts of the deposition tunnels of the SFR is calculated by multiplying the flow values given in the report "Details of predicted flow in deposition tunnels at SFR, Forsmark" R-01-21 /Holmén and Stigsson 2001b/ by the appropriate u-factors as defined in the randomly selected row of the matrix of u-factors.

An example of such a matrix is given below in Table 2-1, considering a future flow situation with the sea at the 2,000 AD level.

Table 2-1. Example of matrix presenting uncertainty factors for 10 accepted realizations. The flow situation represents a future situation with the sea at the 2,000 AD level. The studied case is the base case.

Uncertainty factors					
Rea	**BMA1**	**BLA1**	**BTF1**	**BTF2**	**SILO**
1	4.32	2.01	1.93	1.83	0.83
2	3.72	1.47	1.36	1.27	0.80
3	3.09	0.81	0.71	0.65	1.11
4	3.03	0.92	0.81	0.75	0.95
5	2.63	0.76	0.65	0.61	0.81
6	3.38	1.19	1.08	1.01	0.93
7	3.20	1.18	1.08	1.01	0.76
8	2.66	0.58	0.47	0.43	1.04
9	4.19	1.39	1.23	1.16	1.02
10	5.77	2.59	2.44	2.34	0.80

An example

Let us assume that row 8 (Rea 8) is randomly selected by the transport model for a certain realisation of the transport model, and that we want to calculate the flow entering a part of the BMA tunnel from South for a future flow situation with the sea at the 2,000 AD level.

1. The flow of a certain part of the BMA tunnel is read in R-01-21 (e.g. 0.25 m^3/year).
2. The flow read in R-01-21 is multiplied by the appropriate u-factor of row 8.

	Old flow		u-factor		New flow
For the 2,000 AD flow situation:	0.25	×	2.66	=	0.665 m^3/year

It is important to remember that the uncertainty factors (see Chapter 2) are not independent from the flow path data (see Chapter 3). When stochastic calculations are performed by use of a transport model and the data presented in this study is used as input to such calculations, the corresponding uncertainty factors and flow path data should be used. Corresponding data is identified by the number of the row in the matrix of uncertainty factors and the number of the files providing flow path data. Hence, the first row with uncertainty factors should be used together with the flow path data files denoted with number 1, and so on.

3 Flow paths

3.1 Flow paths: Methodology

Flow paths from the deposition tunnels of the SFR are presented in /Holmén and Stigsson 2001a/ for different levels of the sea, and for different cases. These paths are calculated for a rock mass with properties as defined by the "old" calibration of the SFR model.

The SFR inverse modelling project /Holmén 2005/ was based on a stochastic description of the properties of the rock mass and of the fracture zones. The properties of the rock mass of the accepted realisation stemming from the SFR-inverse project /Holmén 2005/ may be very different form the properties of the rock mass of the /Holmén and Stigsson 2001ab/ model.

The different accepted realisations of the SFR-inverse modelling project produce approximately the same inflow to the SFR tunnels when simulating drained tunnels; nevertheless the properties of the flow paths (distribution of values of breakthrough time and length) for the future situations (2,000 AD and 5,000 AD) may be rather different for the different accepted realisations because the properties of the fracture zones (and rock mass) will be different for different realisations.

It is therefore necessary to calculate new flow paths from the SFR tunnels for each of the accepted realisations of the SFR-inverse project and for the two sea water levels studied (2,000 AD and 5,000 AD).

It was proposed at the meeting at SKB (06-10-12) that a single value of the effective porosity should be used for all fracture zones and rock masses within the model when the new flow paths are simulated. The purpose of using a single value of effective porosity is that it will be possible to back-calculate an F-factor that is reasonable for the studied system and comparable to the values used by SKB in other studies (the F-factor is defined as the flow wetted surface area divided by the flow). When the flow paths of this study were simulated, the effective porosity of the rock mass and the fracture zones was set to 0.005.

In this study the flow pattern of the groundwater is analysed by use of flow paths. The groundwater flow model used for calculating the groundwater flow in the deposition tunnels and in the surrounding rock mass (GEOAN , see /Holmén 1992, 1997/) also has the capability to create flow paths by simulating the movement of particles; particles that follow the flow of groundwater through the model (i.e. particle tracking). The simulation of the movement of particles inside the computational cells is based on an analytic method by /Pollock 1989/.

In the models, the flow paths will develop inside a flow field that controls the movements of the paths. The paths are simulated considering a fixed flow field. Two different points in time are studied: 2,000 AD and 5,000 AD. The flow paths were analysed considering two different parameters: length and breakthrough time. This was also done for the overall spatial distribution of discharge points. In this study we have examined advective flow paths only; diffusion, mechanical mixing and retardation were not included in the models studied. Migration modeling will take place in a subsequent study using the results of the current study as input.

As previously stated the flow paths are created by virtual particles that move with the calculated groundwater flow. In the model, the particles (flow paths) are released in a uniform pattern within the numerical cells that represents a deposition tunnel (e.g. the cells of the BMA tunnel). The flow paths will first move with the groundwater flow within the tunnel and after a certain movement inside the tunnel the particles will enter the rock mass and the fracture zones outside of the tunnels.

Examples of flow paths are given in Figure 3-2.

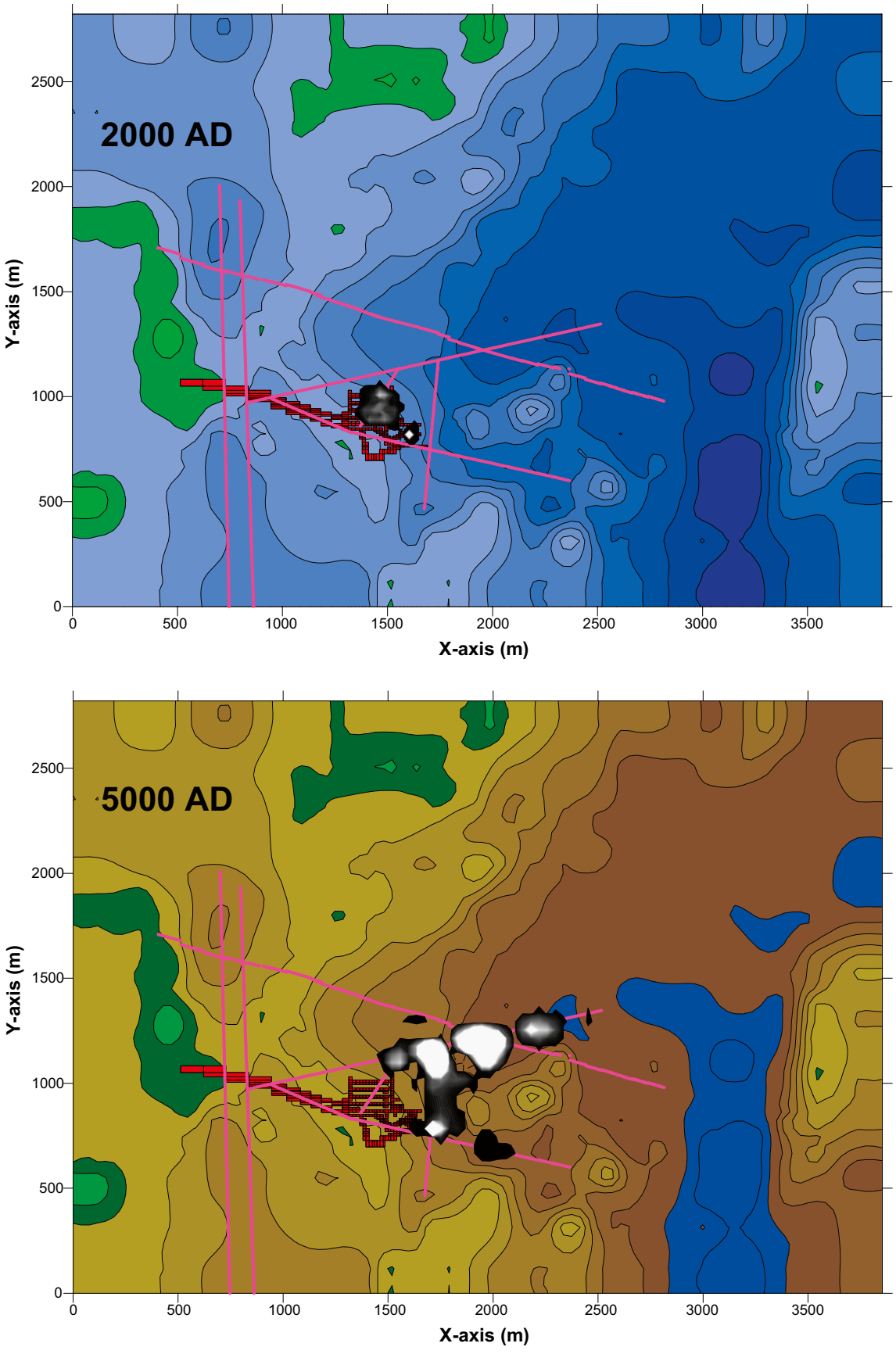

Figure 3-1. *Discharge areas for flow paths from the deposition tunnels (BMA, BLA, BTF1, BTF2 and SILO) for the flow situation at 2,000 AD and 5,000 AD. Discharge points are calculated for each one of the 60 accepted realizations studied. The discharge areas are represented by the black-white clouds. (Areas located below the sea are marked with blue colours.)*

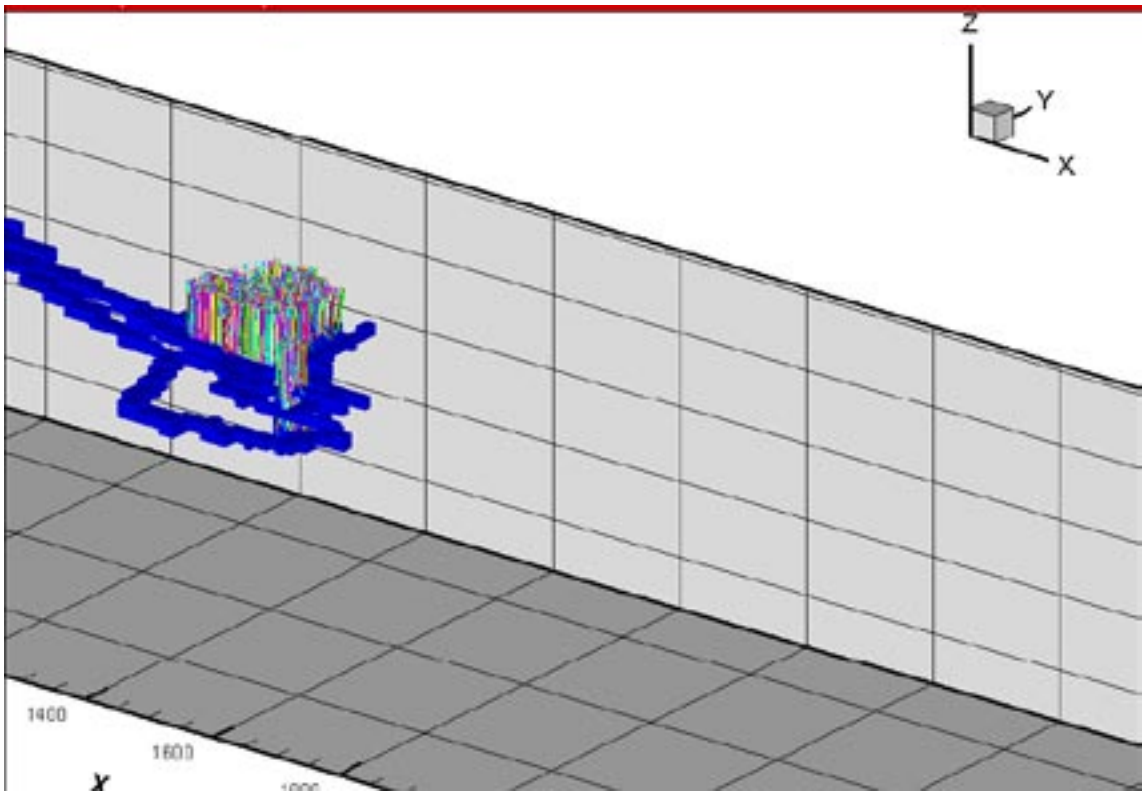

(i) Flow paths at 2,000 AD (Rea 29)

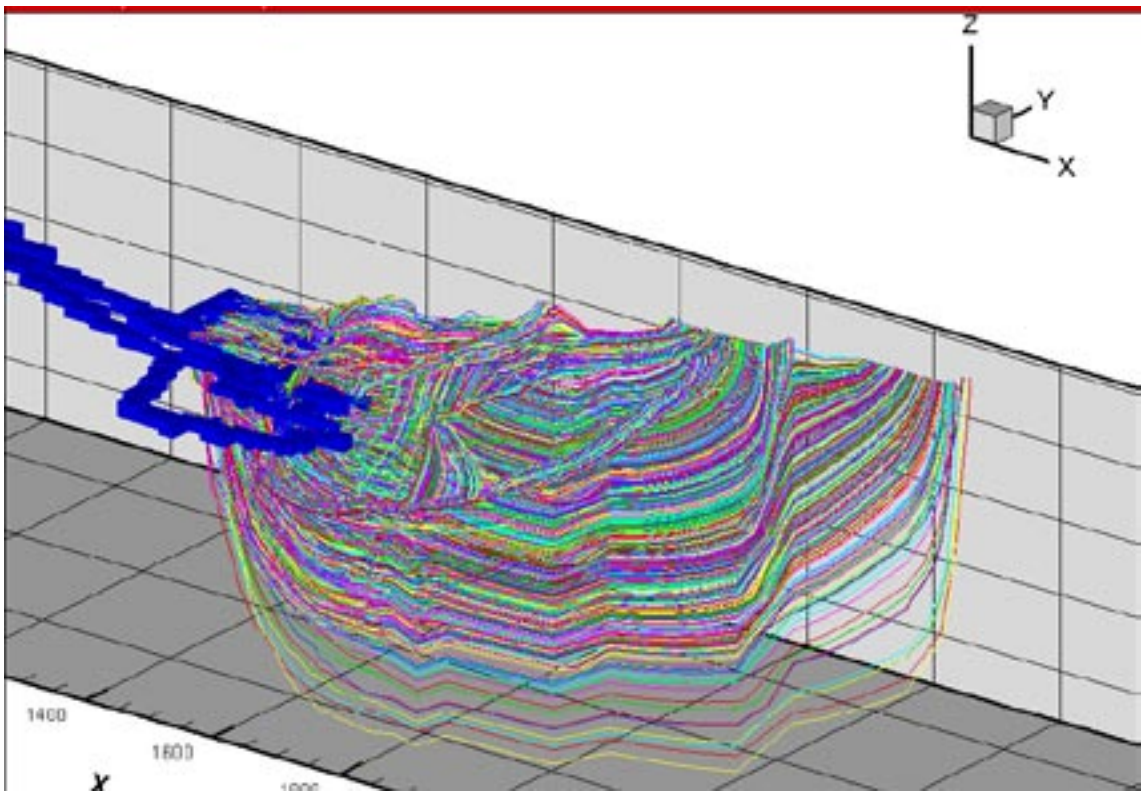

(i) Flow paths at 5,000 AD (Rea 29)

Figure 3-2. *Visualization of flow paths from the deposition tunnels.*

The data that will be exported to the transport modelling is length and breakthrough time for the movement *outside* of the tunnel. The purpose of releasing the particles in a uniform pattern inside the tunnels and to simulate the movement inside the tunnels is to create a good spatial distribution of the paths when they enter the rock mass. The release positions are important because the spatial distribution of the flow paths as they enter the rock is very heterogeneous, which is well demonstrated by Figure 3-3. The release of the particles is not flow-weighted.

Figure 3-3 represents a randomly selected realization and presents a visualisation of the flow paths from the BMA tunnel. The studied flow situation is situation with a closed repository with resaturated tunnels, and with the sea at the 2,000 AD level. As seen in the figure and for the BMA tunnel, most particles will enter the rock at the position where Zone 6 intersects the tunnel, i.e. most flow paths from the tunnel will enter zone 6 and not the rock mass that surrounds zone 6.

Length and breakthrough time of flow paths varies significantly within a realisation, but also between realisations.

As previously discussed in Section 1.2, the discharge points of the flow paths have a tendency to follow the retreating shoreline, even after the time when flows of the tunnels have reached a steady state similar situation. At 4,000 AD the shore line is at a certain distance form the tunnels, but the shoreline is still retreating. At 5,000 AD, a local lake has been created east of the SFR repository and the water level of this lake is steady (in the model); at 5,000 AD the retreat of the shoreline is no longer influencing the flow paths from the deposition tunnels as the water level of the lake is not changing and as the shoreline is far away form the SFR.

The discharge areas for the flow paths studied are presented in Figure 3-1. The figure presents the distribution of flow paths for the 60 accepted realizations, for the two different moments in time studied: 2,000 AD and 5,000 AD. In all 300 000 flow paths are analysed for each figure, which follows from 1,000 paths for each one of the 5 deposition tunnels and for each one of the 60 accepted realisations.

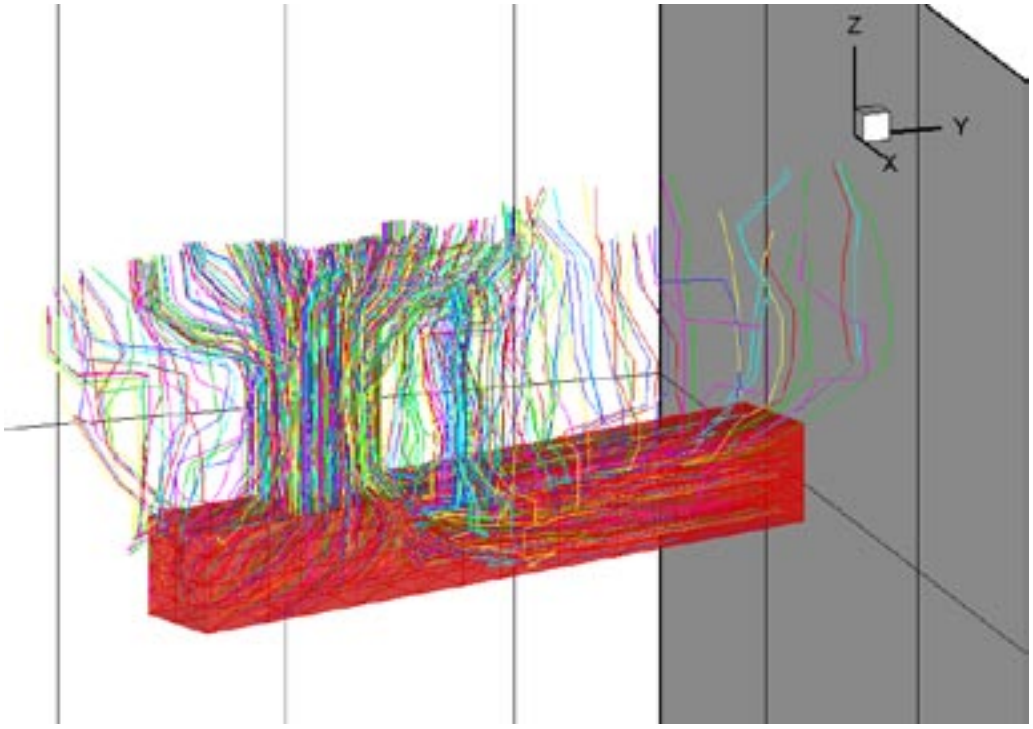

Figure 3-3. *Example of flow paths (multi colour) from the BMA tunnel (red). The groundwater flow corresponds to a future situation with the sea at the 2,000 AD level. For the studied realization most flow paths are concentrated to Zone 6, which intersect the tunnel.*

3.2 Flow paths: General statistics

Statistical analyses have been carried out of the properties of the simulated flow paths, two properties have been studied (i) length of paths and (ii) breakthrough time of the movement of a particle along a flow path (advective movement). The properties of the flow paths will form different statistical distributions when considering the different deposition tunnels and the different realizations.

The statistical distributions discussed below will not necessarily be directly used in the transport modelling; they are presented as a description of the results of the flow path analyses. The results that we expect to be used in the transport modelling are the individual flow paths, as defined by lengths and breakthrough times. See Section 3.4.

Statistical distributions are characterised by percentiles. A percentile is defined as "a value below which a certain percentage of the observations fall". In this study results of statistical analyses are given by use of percentiles.

In this section we will present statistics considering each deposition tunnels separately, but we will consider all flow paths of the 60 accepted realizations as one ensemble of flow paths. Hence, the results given below will include the spread in values (e.g. variation in breakthrough time) caused by:

(i) the heterogeneity of the rock mass (the heterogeneity is defined by the different properties of the rock mass and the fracture zones of an accepted realization),

(ii) the uncertainty in rock mass properties, as represented by the different properties of the 60 accepted realizations.

The results of the statistical analyses are given below in a number of tables and figures:

- The flow situation at 2,000 AD: Table 3-1, Figure 3-4 and Figure 3-5.
- The flow situation at 5,000 AD: Table 3-2, Figure 3-6 and Figure 3-7.

At 2,000 AD, the flow paths are short and directed upward from the deposition tunnels to the sea bed. The groundwater flow is small due to a very small hydraulic gradient and therefore the breakthrough times at 2,000 AD are not short although the lengths are short. At 5,000 AD flow path lengths are larger than at 2,000 AD, but the breakthrough times are shorter. The shorter breakthrough times at 5,000 AD follow from the larger groundwater flow at 5,000 AD; the larger flows follow from the increased hydraulic gradients. This is further discussed in /Holmén and Stigsson 2001a/.

Table 3-1. BMA, BLA, BTF1, BTF2, SILO: Variation in length and breakthrough time of flow paths considering 60 accepted realisation and the flow situation at 2,000 AD. (Effective porosity is equal to 0.005.)

2,000 AD	Length of flow paths (m)				
Percentiles	BMA	BLA	BTF1	BTF2	SILO
1	66.0	71.0	77.0	71.6	61.0
5	66.0	71.0	77.0	77.0	61.0
10	66.1	71.0	77.1	77.0	61.0
20	66.2	71.1	77.1	77.1	66.1
30	66.4	71.2	77.2	77.2	66.1
40	66.6	71.4	77.4	77.3	66.2
50	67.4	71.8	77.9	77.7	66.2
60	68.5	72.7	78.7	78.5	66.4
70	69.8	74.0	79.7	79.6	66.7
80	71.2	75.6	81.0	80.9	78.4
90	73.5	77.6	82.7	82.8	104.0
95	76.2	79.1	84.1	84.2	119.6
99	80.1	81.1	85.7	86.1	132.2
P90–P10	*7.4*	*6.6*	*5.7*	*5.8*	*43.0*

2,000 AD	Breakthrough time of flow paths (years)				
Percentiles	BMA	BLA	BTF1	BTF2	SILO
1	5	3	4	4	216
5	6	4	8	7	243
10	8	6	16	11	284
20	12	9	41	25	335
30	22	14	77	53	384
40	46	22	229	117	432
50	86	40	317	272	495
60	185	66	372	331	561
70	241	187	447	392	613
80	296	277	590	519	738
90	432	407	704	689	1,083
95	539	558	803	760	1,581
99	797	748	936	927	2,681
P90–P10	*424*	*401*	*688*	*678*	*799*

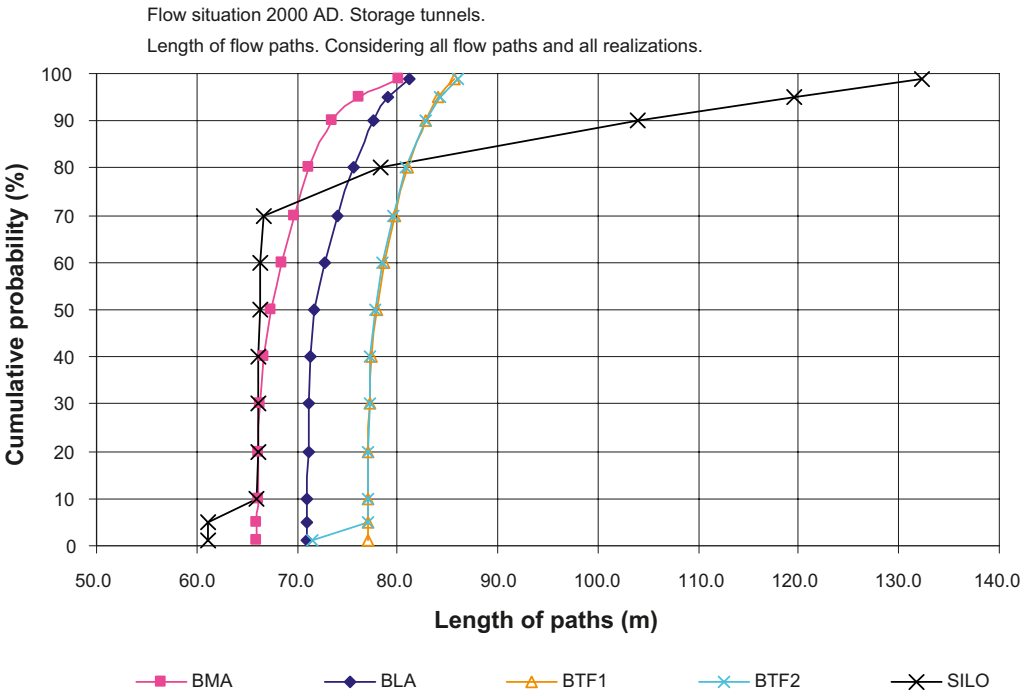

Figure 3-4. *Length of flow paths from deposition tunnels for the flow situation at 2,000 AD.*

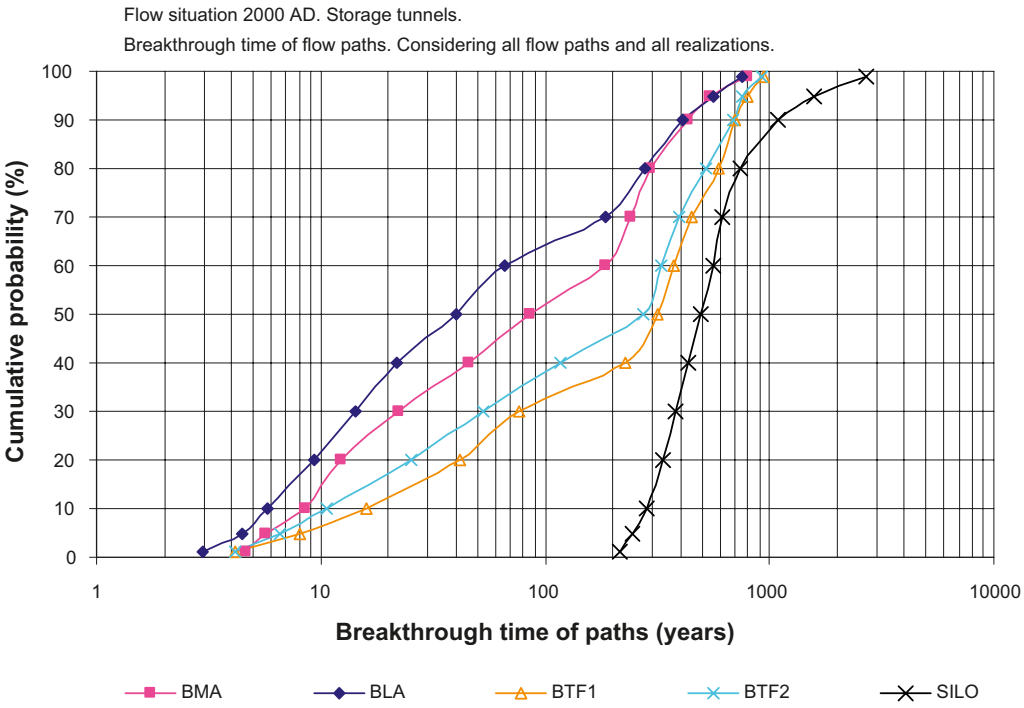

Figure 3-5. *Length of flow paths from deposition tunnels for the flow situation at 2,000 AD.*

Table 3-2. BMA, BLA, BTF1, BTF2, SILO: Variation in length and breakthrough time of flow paths considering 60 accepted realisation and the flow situation at 5,000 AD. (Effective porosity is equal to 0.005.)

5,000 AD	Length of flow paths (m)				
Percentiles	BMA	BLA	BTF1	BTF2	SILO
1	151.1	153.9	114.7	141.2	165.2
5	178.8	194.8	144.7	203.9	169.8
10	237.5	260.9	169.1	249.7	174.5
20	333.4	303.5	224.7	274.9	186.0
30	358.7	350.4	255.9	298.7	303.0
40	383.6	410.7	286.9	334.6	356.5
50	425.0	503.4	314.8	412.1	387.9
60	551.0	574.4	380.0	515.0	436.2
70	608.6	621.5	498.1	590.5	707.4
80	670.6	699.3	582.6	709.9	784.8
90	748.6	812.6	940.9	944.4	891.0
95	814.7	892.3	1,332.3	1,067.3	990.9
99	984.3	1,010.0	1,557.0	1,283.2	1,148.8
P90–P10	*511*	*552*	*772*	*695*	*716*

5,000 AD	Breakthrough time of flow paths (years)				
Percentiles	BMA	BLA	BTF1	BTF2	SILO
1	4	4	6	5	12
5	6	7	8	7	22
10	8	9	11	9	28
20	11	13	16	12	39
30	14	16	23	18	50
40	17	20	33	25	59
50	22	26	45	36	72
60	29	33	61	50	94
70	41	47	83	70	151
80	58	76	121	115	412
90	91	180	256	247	866
95	119	357	552	476	1,367
99	206	853	1,527	1,122	2,457
P90–P10	*83*	*171*	*245*	*238*	*838*

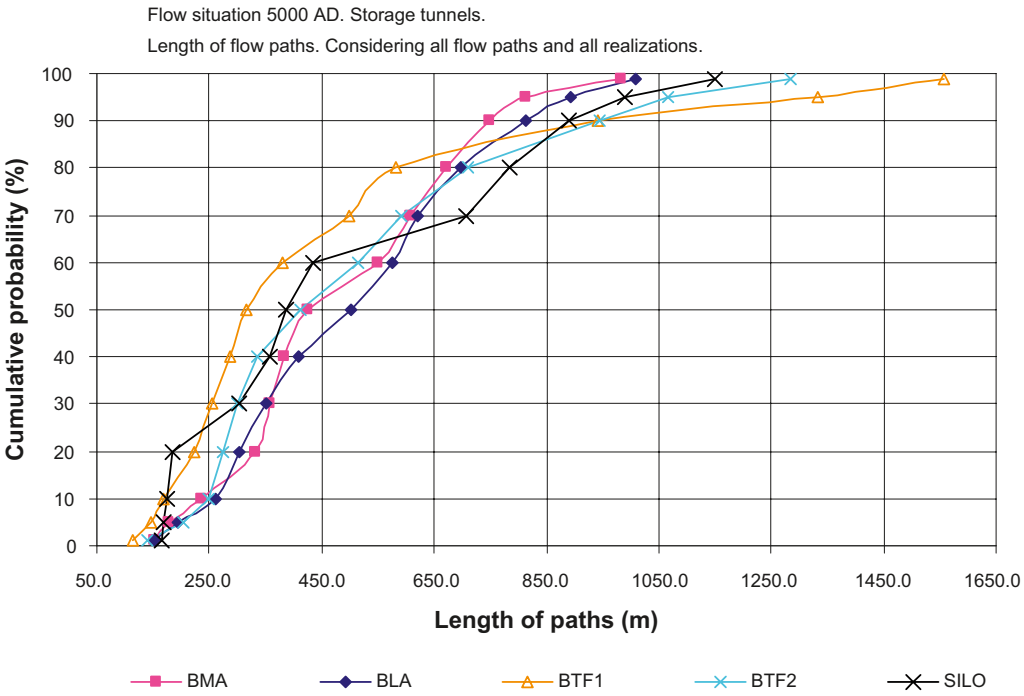

Figure 3-6. *Length of flow paths from deposition tunnels for the flow situation at 5,000 AD.*

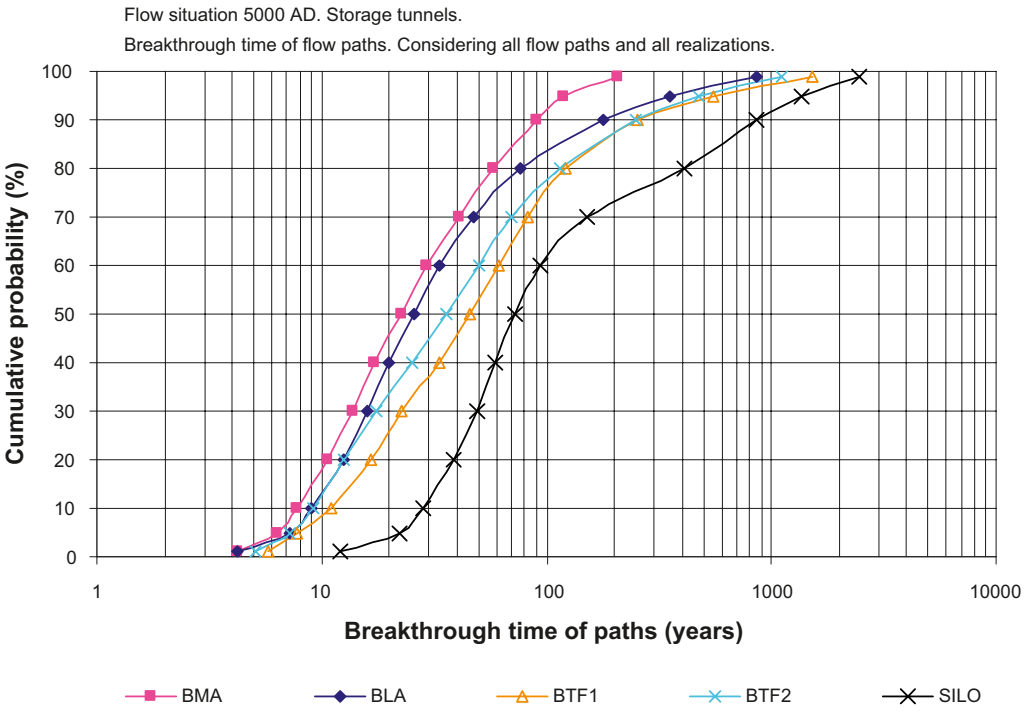

Figure 3-7. *Length of flow paths from deposition tunnels for the flow situation at 5,000 AD.*

3.3 Flow paths: Variation of lengths and breakthrough times within and between accepted realisations

3.3.1 Variations: 2,000 AD

There is a significant variation in path breakthrough time both within an accepted realization and between accepted realizations. To illustrate these variations different statistical modes of the path data have been compared for the accepted realizations. The comparison refers to the 10th percentil, the 50th percentile (the median) and the 90th percentile of the path data for each accepted realization.

To be able to calculate the variation in flow paths statistics between different accepted realizations, flow paths must be simulated and analyzed for each accepted realization separately.

Hence

- For each realization studied, 1,000 flow paths have been simulated with start points inside the deposition tunnels studied. Flow path data have been calculated considering the movement outside of the tunnels.
- For each realization studied, statistics (percentiles) have been calculated for the path data.
- The calculated percentiles are presented in Table 3-3. For the BMA and the SILO the results are also given in Figure 3-8 through Figure 3-11.

It is seen in Figure 3-8 (and in Table 3-3) that the median of the path lengths, outside of the BMA tunnel, varies from 66 m to approximately 71 m. The 90th percentile of the path lengths varies from 70 m to approximately 77 m. These are small variations and follow from the geometry of the studied tunnel, Zone 6 and the level of the sea. Or in other words: Since the groundwater flow at 2,000 AD is primarily upwards and the vertical distance between the sea and the BMA tunnel is the same, regardless of the permeability of the rock, the variation in length of flow paths will be very small.

It is seen in Figure 3-9 (and in Table 3-3) that the median of the path breakthrough time, outside of the BMA tunnel, varies from 5 years and up to approximately 360 years. The 90th percentile of the path breakthrough times varies from 180 years and up to approximately 830 years. These are large variations and follow from the different values of permeability of the rock. Or in other words: Even if the length of the flow paths are very much the same, the different permeability values of fracture zones and rock mass will lead to a large variation in the breakthrough time of the flow paths.

Considering all five deposition tunnels and the flow situation at 2,000 AD, a summary of the statistics of path length and breakthrough time is given in Table 3-3. Examples of how to interpret Table 3-3 follows below:

- For the BMA there is with a probability of 10% (10th percentile) realizations in which the shortest 10% (Tp10) of the breakthrough times are smaller than 6 years.
- For the BMA there is with a probability of 10% (90th percentile) realizations in which the shortest 10% (Tp10) of the breakthrough times are larger than 34 years.
- For the BMA there is with a probability of 10% (10th percentile) realizations in which the median (Tp50) of the breakthrough times are smaller than 7 years.
- For the BMA there is with a probability of 10% (90th percentile) realizations in which the median (Tp50) of the breakthrough times are larger than 243 years.
- For the BMA there is with a probability of 10% (10th percentile) realizations in which the longest 10% (Tp90) of the breakthrough times are smaller than 217 years.
- For the BMA there is with a probability of 10% (90th percentile) realizations in which the longest 10% (Tp90) of the breakthrough times are larger than 575 years.

We may define the variation of values, or spread of values (a measure of the variance) as the difference between the 90th percentile and the 10th percentile of the distribution of values studied.

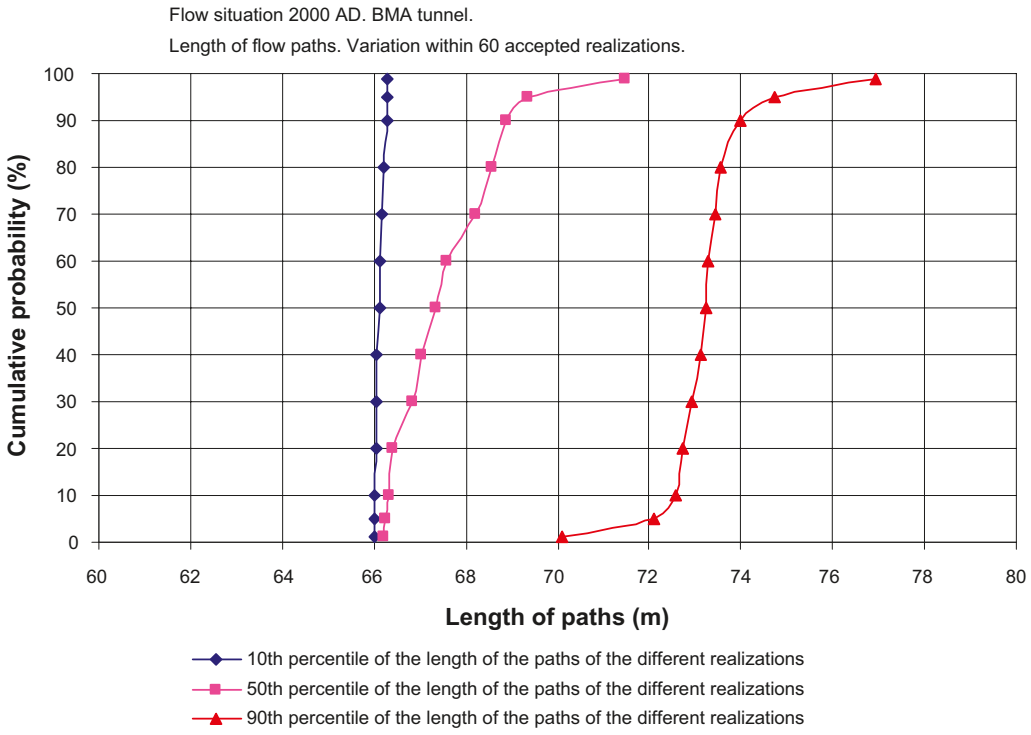

Figure 3-8. *Variation of path length within 60 accepted realizations, considering the BMA tunnel and a future flow situation with the sea at the 2,000 AD level.*

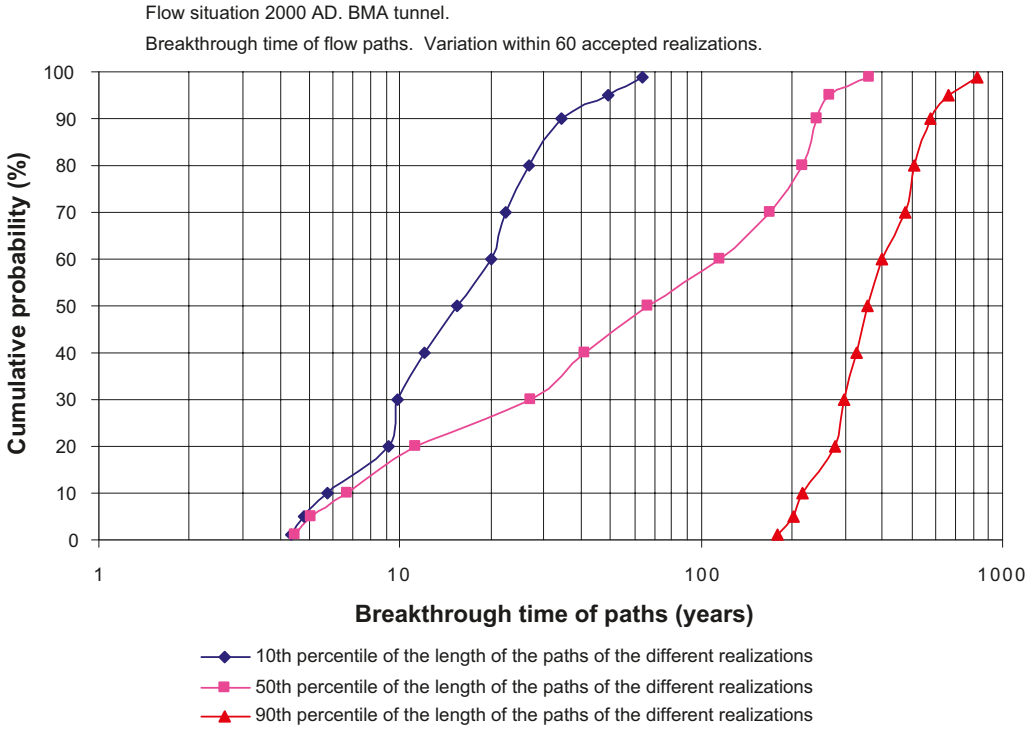

Figure 3-9. *Variation of path breakthrough time within 60 accepted realizations, considering the BMA tunnel and a future flow situation with the sea at the 2,000 AD level.*

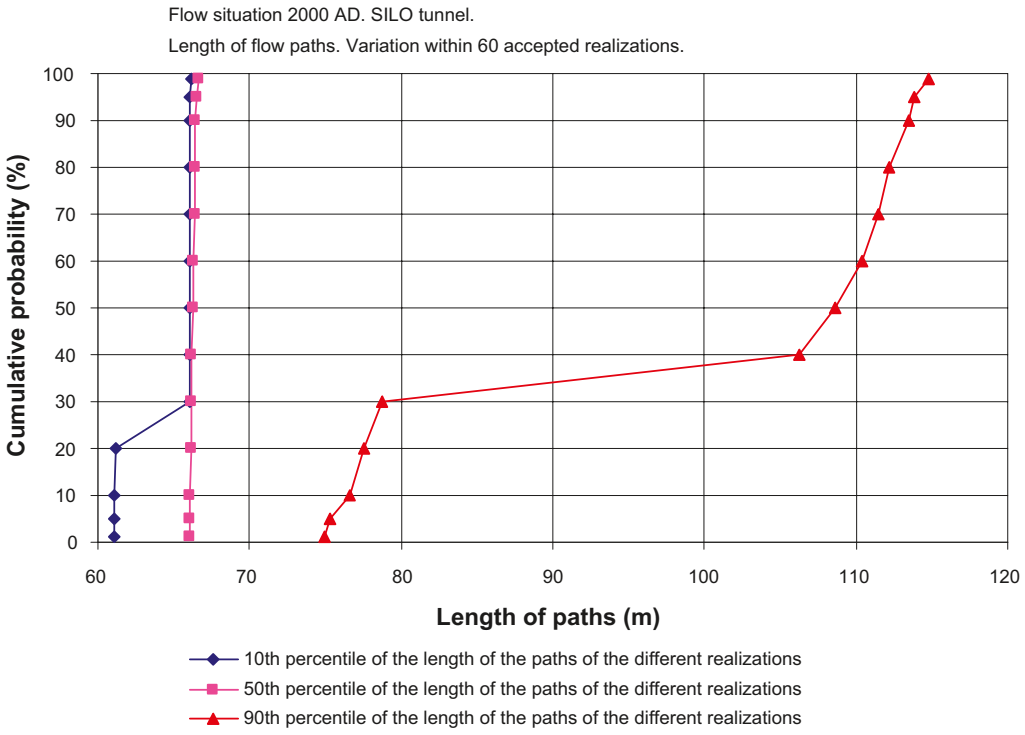

Figure 3-10. *Variation of path length within 60 accepted realizations, considering the. SILO and a future flow situation with the sea at the 2,000 AD level.*

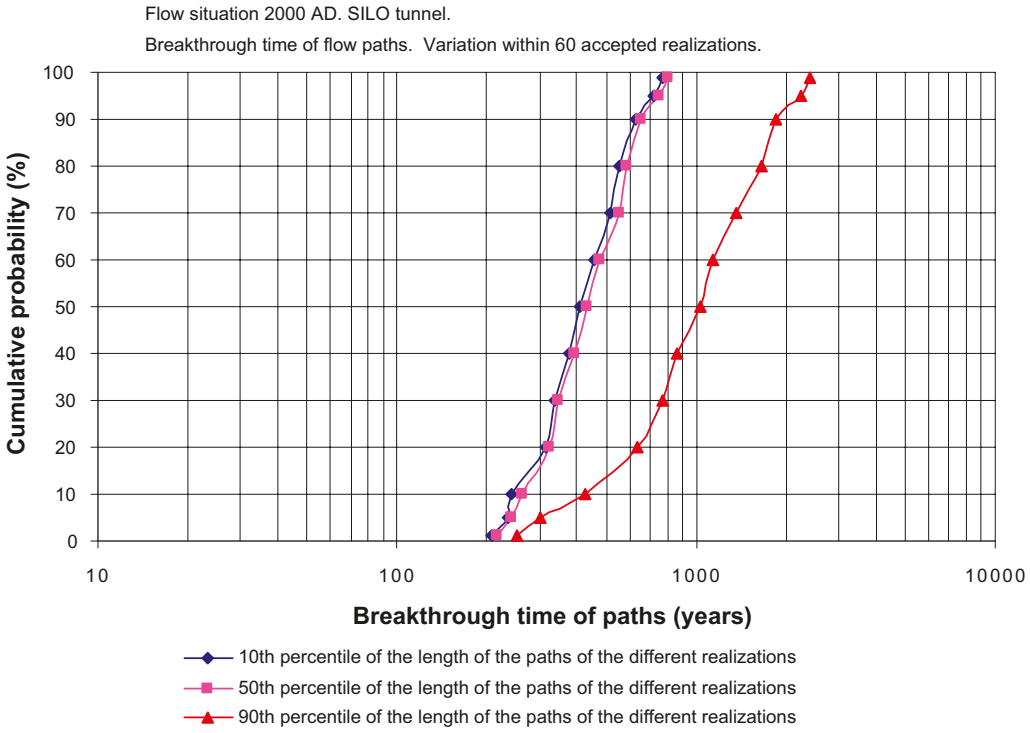

Figure 3-11. *Variation of path breakthrough time within 60 accepted realizations, considering the SILO tunnel and a future flow situation with the sea at the 2,000 AD level.*

Table 3-3. BMA, BLA, BTF1, BTF2, SILO: Variation in length and breakthrough time of flow paths considering the 60 accepted realisation. The groundwater flow situation represents a future flow situation with the sea at the 2,000 AD elevation.

Lp10, Lp50, Lp90 denotes the 10th , 50th , 90th percentiles of the flow path length distribution of an accepted realization.

Tp10, Tp50, Tp90 denotes the 10th , 50th , 90th percentiles of the flow path breakthrough time distribution of an accepted realization.

p90–p10 denotes the difference between the p90 and the p10 value, as an independent distribution.

Note, that all values in the horizontal rows are independent, hence they do not necessarily come from the same realization.

Length (m)					**Breakthrough time (years)**				
BMA 2000AD					BMA 2000AD				
Percentile	Lp10(m)	Lp50(m)	Lp90(m)	p90-p10	Percentile	Tp10(a)	Tp50(a)	Tp90(a)	p90-p10
1	66.0	66.2	70.1	4.1	1	4	4	179	160
5	66.0	66.3	71.8	5.8	5	5	5	203	168
10	66.0	66.3	72.6	6.4	10	6	7	217	184
20	66.0	66.4	72.7	6.7	20	9	11	279	250
30	66.1	66.9	72.9	6.8	30	10	27	299	278
40	66.1	67.0	73.1	7.0	40	12	41	327	304
50	66.1	67.4	73.2	7.1	50	15	67	356	351
60	66.1	67.6	73.3	7.2	60	20	115	400	387
70	66.2	68.2	73.4	7.3	70	22	169	478	463
80	66.2	68.5	73.6	7.4	80	27	217	512	500
90	66.3	68.9	74.0	7.8	90	34	243	575	568
95	66.3	69.4	74.7	8.5	95	49	266	660	648
99	66.3	71.5	76.9	10.8	99	64	363	828	810
BLA 2000AD									
Percentile	Lp10(m)	Lp50(m)	Lp90(m)	p90-p10	Percentile	Tp10(a)	Tp50(a)	Tp90(a)	p90-p10
1	71.0	71.1	75.4	4.2	1	2	4	192	172
5	71.0	71.1	75.8	4.6	5	3	5	206	179
10	71.0	71.2	76.0	4.8	10	4	6	222	201
20	71.0	71.3	76.9	5.7	20	5	9	288	264
30	71.0	71.5	77.3	6.2	30	6	13	311	294
40	71.1	71.7	77.4	6.4	40	8	20	340	327
50	71.1	71.8	77.8	6.8	50	11	28	389	374
60	71.1	72.0	77.9	6.8	60	13	39	449	444
70	71.1	72.3	78.1	7.0	70	16	48	526	520
80	71.2	72.4	78.2	7.2	80	22	67	564	559
90	71.2	72.5	78.4	7.4	90	29	177	639	626
95	71.2	72.6	78.6	7.5	95	40	216	711	702
99	71.2	72.8	78.7	7.6	99	52	249	771	760
BTF1 2000AD					BTF1 2000AD				
Percentile	Lp10(m)	Lp50(m)	Lp90(m)	p90-p10	Percentile	Tp10(a)	Tp50(a)	Tp90(a)	p90-p10
1	77.0	77.3	79.6	2.6	1	3	72	224	193
5	77.0	77.4	80.2	3.1	5	4	90	232	200
10	77.0	77.5	80.7	3.6	10	5	135	248	226
20	77.0	77.5	81.4	4.4	20	8	215	334	306
30	77.0	77.6	81.9	4.9	30	9	285	371	349
40	77.1	77.7	82.4	5.3	40	12	319	410	392
50	77.1	77.9	82.8	5.7	50	14	367	468	450
60	77.1	78.0	83.0	6.0	60	20	386	552	544
70	77.1	78.3	83.4	6.3	70	21	486	656	634
80	77.1	78.6	83.9	6.9	80	27	608	719	714
90	77.1	78.8	84.1	7.0	90	33	678	790	768
95	77.1	79.0	84.3	7.3	95	47	739	913	900
99	77.1	79.2	84.7	7.7	99	59	901	973	956

Length (m)					Breakthrough time (years)				
BTF2 2000AD					BTF2 2000AD				
Percentile	Lp10(m)	Lp50(m)	Lp90(m)	p90-p10	Percentile	Tp10(a)	Tp50(a)	Tp90(a)	p90-p10
1	72.8	77.2	79.6	2.5	1	4	52	219	195
5	76.8	77.3	80.2	3.1	5	4	62	231	199
10	77.0	77.4	80.7	3.6	10	5	73	249	219
20	77.0	77.5	81.7	4.7	20	8	127	329	304
30	77.0	77.5	82.3	5.3	30	9	214	367	345
40	77.0	77.7	82.7	5.7	40	11	269	401	386
50	77.0	77.7	83.1	6.2	50	14	311	459	441
60	77.1	77.8	83.3	6.4	60	18	344	543	535
70	77.1	77.9	83.6	6.6	70	21	372	635	614
80	77.1	78.2	83.8	6.8	80	27	446	697	692
90	77.1	78.6	84.1	7.2	90	33	639	774	753
95	77.1	78.7	84.3	7.5	95	47	711	868	854
99	77.1	78.8	84.7	9.2	99	61	817	942	927
SILO 2000AD					SILO 2000AD				
Percentile	Lp10(m)	Lp50(m)	Lp90(m)	p90-p10	Percentile	Tp10(a)	Tp50(a)	Tp90(a)	p90-p10
1	61.0	66.0	74.9	11.0	1	208	216	252	43
5	61.1	66.1	75.3	13.4	5	236	243	301	60
10	61.1	66.1	76.6	15.3	10	242	262	429	111
20	61.2	66.1	77.5	16.4	20	313	325	639	207
30	66.0	66.2	78.7	17.6	30	335	348	776	354
40	66.0	66.2	106.3	40.3	40	378	390	864	545
50	66.0	66.3	108.6	42.6	50	408	433	1032	676
60	66.0	66.3	110.4	44.3	60	454	477	1132	754
70	66.1	66.3	111.5	45.5	70	515	551	1364	928
80	66.1	66.4	112.1	46.1	80	556	585	1652	1114
90	66.1	66.4	113.5	47.4	90	630	656	1851	1221
95	66.1	66.5	113.8	47.8	95	719	747	2249	1526
99	66.1	66.6	114.8	48.7	99	768	809	2405	1668

Variation within an accepted realization

Considering a variation in flow path properties within an accepted realization, the variation is defined as the difference between the 90th percentile and the 10th percentile of the distribution of values studied within a realization. Each realization will produce one value of the studied parameter. Such a variation is presented in Table 3-3 as the values given in the “p90–p10” columns. For the BMA the median variation in breakthrough time is 351 years.

Variation between accepted realizations

Considering a variation in flow path properties between accepted realizations, such a variation may be calculated based on the spread of a certain statistical mode when comparing the distributions. For example, each accepted realization will produce one median value of the studied parameter, e.g. median breakthrough time. Variation between realizations may be defined as the difference between the 90th percentile and the 10th percentile of the distribution of median values as given by the ensemble of accepted realizations. Such a variation can be easily calculated from Table 3-3 as the differences between the 90th and 10th percentile along the vertical columns of values. For the BMA the variation in median breakthrough time (Tp50), when considering the differences between the 90th and 10th percentile is 243–7 = 236 years.

A comparison of the size of variation is given in Section 3.3.3 and in Table 3-5.

3.3.2 Variations: 5,000 AD

The variation in path lengths and breakthrough times between accepted realizations, at 5,000 AD, is discussed below. The methodologies for these analyses were the same as discussed in the previous section (Section 3.3.1).

Considering all five deposition tunnels and the flow situation at 2,000 AD, a summary of the statistics of path length and breakthrough time is given in Table 3-4, results for the BMA and SILO tunnels are also given in Figure 3-12 through Figure 3-15.

Examples of how to interpret Table 3-4 follows below:

- For the SILO there is with a probability of 10% (10th percentile) realizations in which the shortest 10% (Tp10) of the breakthrough times are smaller than 18 years.
- For the SILO there is with a probability of 10% (90th percentile) realizations in which the shortest 10% (Tp10) of the breakthrough times are larger than 81 years.
- For the SILO there is with a probability of 10% (10th percentile) realizations in which the median (Tp50) of the breakthrough times are smaller than 29 years.
- For the SILO there is with a probability of 10% (90th percentile) realizations in which the median (Tp50) of the breakthrough times are larger than 750 years.
- For the SILO there is with a probability of 10% (10th percentile) realizations in which the longest 10% (Tp90) of the breakthrough times are smaller than 59 years.
- For the SILO there is with a probability of 10% (90th percentile) realizations in which the longest 10% (Tp90) of the breakthrough times are larger than 1,244 years.

As previously discussed, we may define the variation of values, or spread of values (a measure of the variance) as the difference between the 90th percentile and the 10th percentile of the distribution of values studied.

Variation within an accepted realization

Considering a variation in flow path properties within an accepted realization, the variation is defined as the difference between the 90th percentile and the 10th percentile of the distribution of values studied within a realization. Each realization will produce one value of the studied parameter. Such a variation is presented in Table 3-4 as the values given in the “p90–p10” columns. For the SILO the median variation in breakthrough time is 249 years.

Variation between accepted realizations

Considering a variation in flow path properties between accepted realizations, such a variation may be calculated based on the spread of a certain statistical mode when comparing the distributions. For example, each accepted realization will produce one median value of the studied parameter e.g. median breakthrough time. Variation between realizations may be defined as the difference between the 90th percentile and the 10th percentile of the distribution of median values as given by the ensemble of accepted realizations. Such a variation can easily be calculated from Table 3-4 as the differences between the 90th and 10th percentile along the vertical columns of values. For the SILO the variation in median breakthrough time (Tp50), when considering the differences between the 90th and 10th percentile, is 750–29 = 721 years.

A comparison of the size of variation is given in Section 3.3.3 and in Table 3-5.

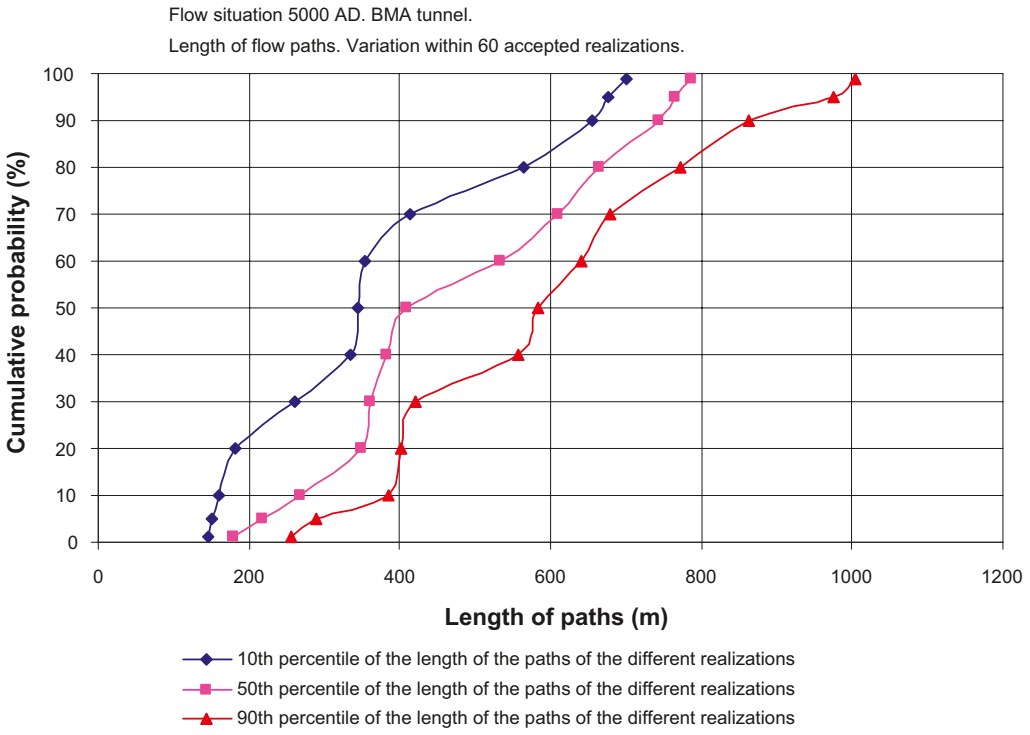

Figure 3-12. *Variation of path length within 60 accepted realizations. BMA tunnel and a future flow situation with the sea at the 5,000 AD level.*

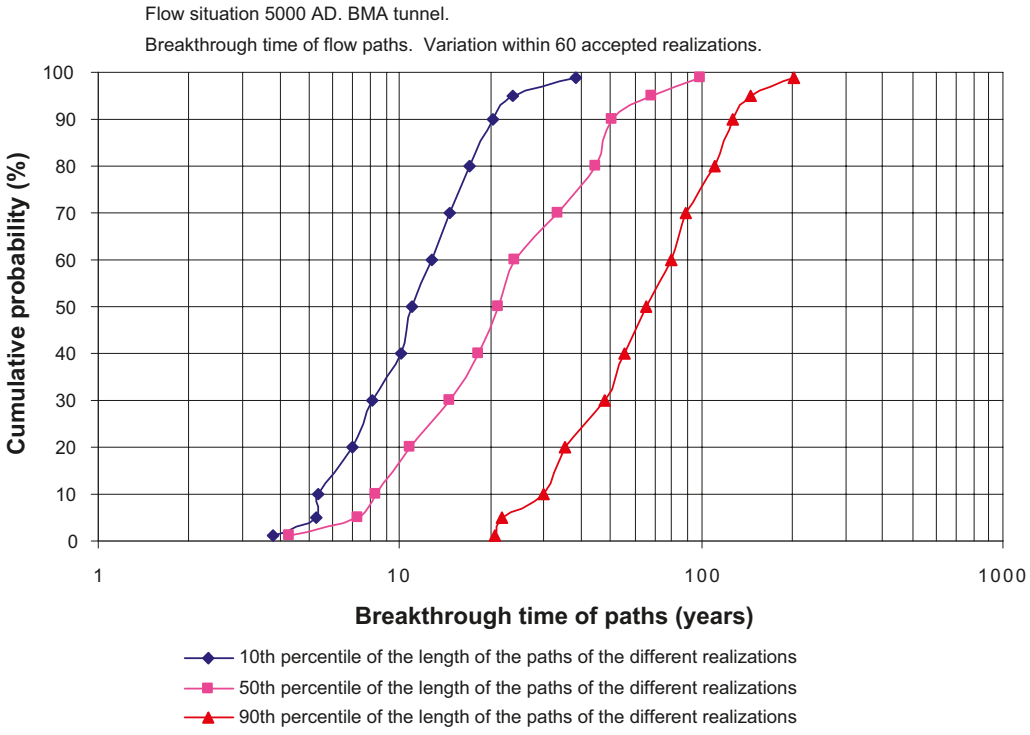

Figure 3-13. *Variation of path breakthrough time within 60 accepted realizations. BMA tunnel and a future flow situation with the sea at the 5,000 AD level.*

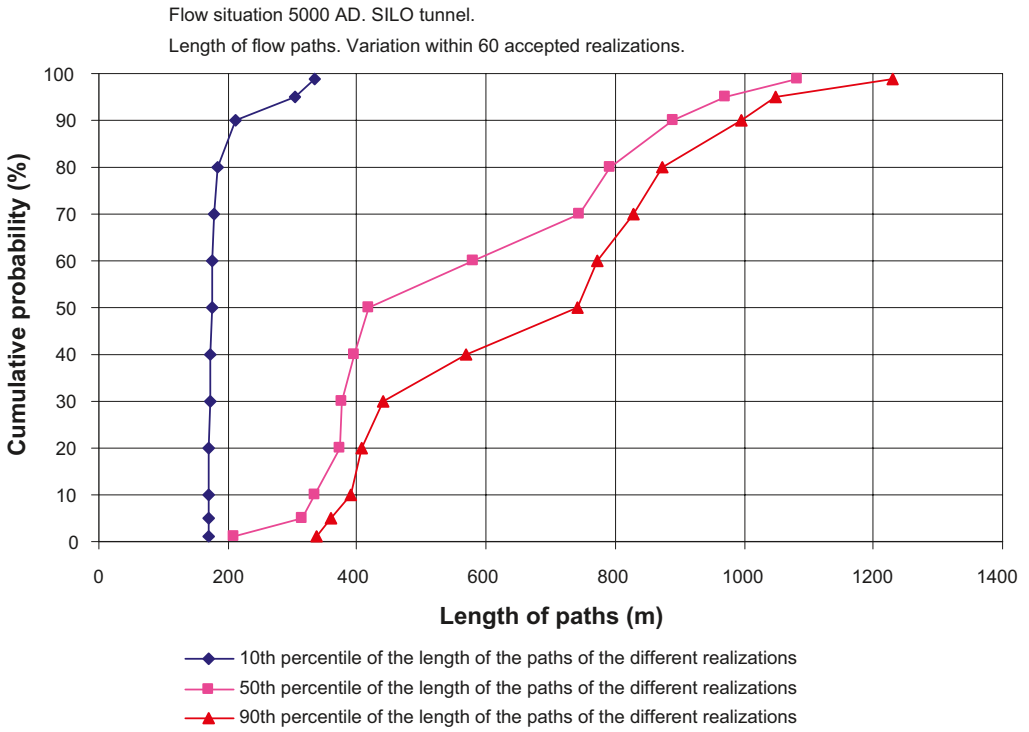

Figure 3-14. *Variation of path length within 60 accepted realizations. SILO tunnel and a future flow situation with the sea at the 5,000 AD level.*

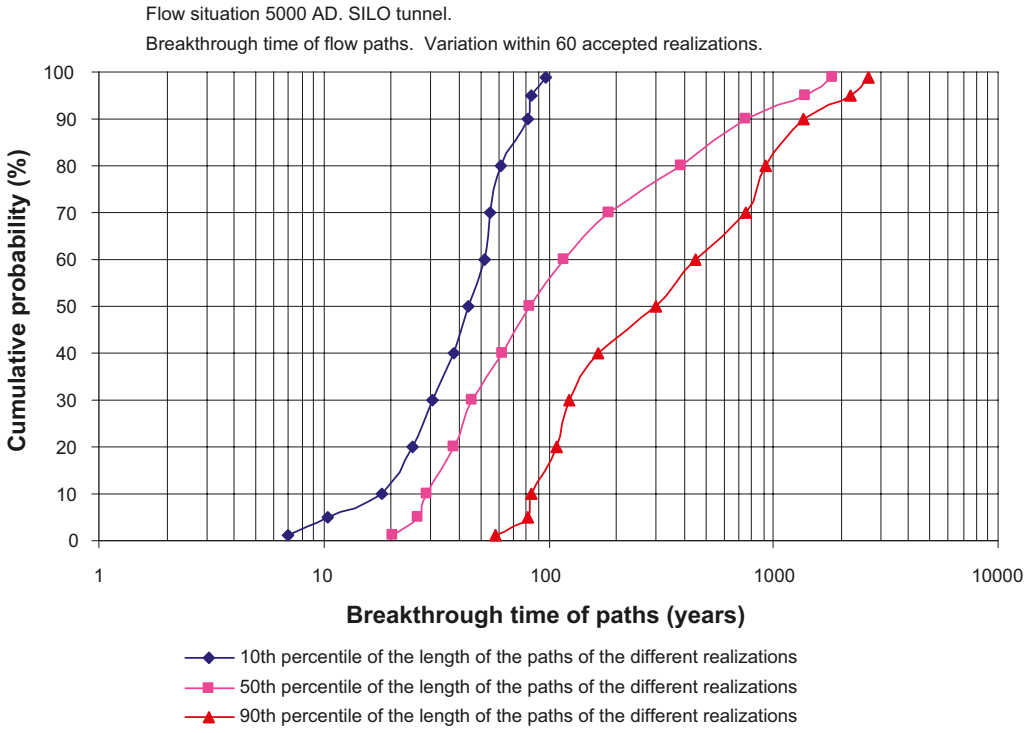

Figure 3-15. *Variation of path breakthrough time within 60 accepted realizations. SILO tunnel and a future flow situation with the sea at the 5,000 AD level.*

Table 3-4. BMA, BLA, BTF1, BTF2, SILO: Variation in length and breakthrough time of flow paths considering the 60 accepted realisation. The groundwater flow situation represents a future flow situation with the sea at the 5,000 AD elevation.

Lp10, Lp50, Lp90 denotes the 10th , 50th , 90th percentiles of the flow path length distribution of an accepted realization.

Tp10, Tp50, Tp90 denotes the 10th , 50th , 90th percentiles of the flow path breakthrough time distribution of an accepted realization.

p90–p10 denotes the difference between the p90 and the p10 value, as an independent distribution.

Note, that all values in the horizontal rows are independent, hence they do not necessarily come from the same realization.

Length (m)

BMA 5000AD

Percentile	Lp10(m)	Lp50(m)	Lp90(m)	p90-p10
1	145.3	179.9	256.3	61.2
5	149.9	218.3	289.0	105.9
10	160.3	267.6	384.9	123.9
20	182.4	349.4	402.6	174.5
30	260.2	362.1	421.1	199.3
40	334.1	381.4	556.6	214.4
50	343.2	408.7	584.3	226.1
60	353.2	532.8	639.5	234.0
70	414.4	609.8	678.9	261.1
80	565.0	663.8	772.4	288.0
90	655.2	744.5	861.8	316.9
95	675.8	765.0	975.3	327.5
99	700.4	787.0	1005.2	359.5

BLA 5000AD

Percentile	Lp10(m)	Lp50(m)	Lp90(m)	p90-p10
1	154.1	269.8	460.5	210.5
5	157.9	292.0	467.8	291.7
10	168.0	310.1	512.4	328.1
20	191.1	332.7	608.8	354.8
30	225.6	368.8	636.0	378.2
40	260.3	403.8	686.6	419.1
50	277.8	490.0	715.5	431.7
60	301.2	538.9	774.3	450.7
70	320.5	590.9	811.0	467.1
80	380.5	623.2	869.5	493.3
90	550.1	654.6	926.9	518.6
95	575.5	806.9	1000.6	525.0
99	599.7	857.7	1009.5	583.2

BTF1 5000AD

Percentile	Lp10(m)	Lp50(m)	Lp90(m)	p90-p10
1	110.1	172.4	279.1	169.0
5	121.0	188.8	351.9	214.6
10	129.0	196.8	485.6	286.1
20	139.9	247.5	552.1	375.0
30	168.7	270.5	642.2	409.5
40	194.9	288.0	709.7	475.3
50	217.5	308.0	778.7	604.9
60	229.4	328.1	1005.1	790.2
70	247.8	356.4	1139.5	954.9
80	267.8	477.5	1322.5	1109.5
90	290.2	564.0	1421.6	1170.9
95	339.4	591.3	1466.4	1188.4
99	396.9	657.6	1512.6	1214.9

Breakthrough time (years)

BMA 5000AD

Percentile	Tp10(a)	Tp50(a)	Tp90(a)	p90-p10
1	4	4	21	13
5	5	7	22	18
10	5	8	30	23
20	7	11	35	29
30	8	15	48	35
40	10	18	56	43
50	11	21	65	49
60	13	24	79	66
70	15	33	89	73
80	17	45	110	99
90	20	51	126	114
95	24	68	147	126
99	39	99	202	185

BLA 5000AD

Percentile	Tp10(a)	Tp50(a)	Tp90(a)	p90-p10
1	4	6	40	31
5	4	10	61	57
10	6	11	83	78
20	8	16	105	91
30	9	20	119	108
40	10	21	141	128
50	12	24	173	163
60	12	28	185	178
70	14	33	219	204
80	15	36	232	217
90	17	48	318	301
95	19	54	418	403
99	22	64	577	566

BTF1 5000AD

Percentile	Tp10(a)	Tp50(a)	Tp90(a)	p90-p10
1	6	7	61	55
5	6	8	72	65
10	7	15	97	84
20	8	18	122	109
30	10	25	146	129
40	13	36	170	152
50	16	43	218	202
60	19	48	256	221
70	22	61	320	309
80	26	69	390	369
90	36	84	406	383
95	40	93	470	423
99	48	112	527	500

Length (m)					Breakthrough time (years)				
BTF2 5000AD					BTF2 5000AD				
Percentile	Lp10(m)	Lp50(m)	Lp90(m)	p90-p10	Percentile	Tp10(a)	Tp50(a)	Tp90(a)	p90-p10
1	140.6	194.0	449.2	209.7	1	4	7	65	57
5	144.8	249.1	489.3	228.0	5	5	11	75	69
10	168.9	272.7	575.8	326.9	10	6	13	98	89
20	232.2	291.0	684.3	419.3	20	7	19	122	110
30	248.9	314.0	745.3	532.3	30	8	21	155	145
40	254.1	333.8	809.3	600.5	40	10	30	176	160
50	262.7	366.2	875.4	620.3	50	11	35	209	191
60	270.2	414.9	947.0	647.0	60	12	38	255	237
70	280.7	475.3	1007.6	678.5	70	14	41	284	270
80	304.5	538.4	1049.8	726.7	80	18	55	319	289
90	453.4	585.0	1107.0	750.9	90	24	67	361	356
95	591.7	706.9	1247.0	760.1	95	31	88	532	514
99	634.1	744.8	1265.3	799.2	99	37	108	682	672
SILO 5000AD					SILO 5000AD				
Percentile	Lp10(m)	Lp50(m)	Lp90(m)	p90-p10	Percentile	Tp10(a)	Tp50(a)	Tp90(a)	p90-p10
1	169.1	209.2	336.3	42.6	1	7	20	58	23
5	169.2	314.8	360.2	62.3	5	10	26	81	48
10	169.4	335.4	390.3	169.0	10	18	29	85	59
20	170.4	372.8	405.8	232.6	20	25	38	108	88
30	171.7	377.8	440.9	264.5	30	31	46	124	101
40	172.4	396.7	568.6	397.6	40	38	62	167	143
50	174.5	418.0	742.4	537.0	50	44	82	302	249
60	176.5	581.2	771.3	593.3	60	52	117	451	392
70	178.8	744.7	828.8	647.3	70	55	186	761	678
80	184.1	793.1	873.9	703.5	80	61	385	917	884
90	213.2	890.4	995.7	818.0	90	81	750	1350	1244
95	304.6	971.0	1049.3	872.7	95	84	1387	2211	2126
99	334.6	1081.4	1229.6	1054.7	99	98	1841	2635	2559

3.3.3 Comparison of variations

As previously discussed in Section 3.3.1 we may define the variation of values, or spread of values (a measure of the variance) as the difference between the 90th percentile and the 10th percentile of the distribution of values studied.

Variation within an accepted realization

Considering a variation in flow path properties within an accepted realization, the variation is defined as the difference between the 90th percentile and the 10th percentile of the distribution of values studied within a realization. Each realization will produce one value describing the variation. A representative value of variation is calculated as the median value of the distributions of variations as given by the ensemble of accepted realizations.

Variation between accepted realizations

Considering a variation in flow path properties between accepted realizations, the variation is calculated based on the spread of median values when comparing the distributions. Each accepted realization will produce one median value of the studied parameter e.g. median breakthrough time. Variation is defined as the difference between the 90th percentile and the 10th percentile of the distribution of median values as given by the ensemble of accepted realizations.

Variation within all flow path data

Considering a variation in flow path properties among all accepted realizations and all flow path data, the variation is defined as the difference between the 90th percentile and the 10th percentile of a distribution of values which contain all flow paths of all accepted realization, i.e., the full ensemble is used.

By use of the approaches discussed above we may compare the variation of values within the different realizations with the variation of values between different realizations and also compare these variations with the total variation when all data is studied as a single data set. Such a comparison is presented in Table 3-5.

By studying flow paths lengths at 2,000 AD, we note that the variation is very small both within the realizations and between the realizations; this is because the flow paths are directed more or less vertically upwards with a minimal spread (see Figure 3-1 , Figure 3-2 and Figure 3-3). However, even if the variations are small, the variations within the realizations are much larger than the variation between realizations.

Table 3-5. Comparison of variation in flow path properties, considering variation within an accepted realization and variation between accepted realizations. Two flow situations are studied: At 2,000 AD and at 5,000 AD.

		Variation in length of flow paths (m)				
		BMA	**BLA**	**BTF1**	**BTF2**	**SILO**
Time: 2,000 AD						
Within a realization	(1)	7	7	6	6	43
Between realizations	(2)	3	1	1	1	5
All paths	(3)	7	7	6	6	43
Time: 5,000 AD						
Within a realization	(1)	266	432	605	620	537
Between realizations	(2)	477	344	367	312	555
All paths	(3)	511	552	772	695	716

		Variation in breakthrough time of flow paths (years)				
		BMA	**BLA**	**BTF1**	**BTF2**	**SILO**
Time: 2,000 AD						
Within a realization	(1)	351	374	450	441	676
Between realizations	(2)	236	171	528	567	394
All paths	(3)	424	401	688	678	799
Time: 5,000 AD						
Within a realization	(1)	49	163	202	191	249
Between realizations	(2)	42	37	69	54	721
All paths	(3)	83	171	245	238	838

(1) Variation is defined as the difference between the 90th percentile and the 10th percentile of the distribution of values studied within an accepted realization. Each realization will produce one value of variation. The variation values given in the table above are median values of the distributions of variations as given by the ensemble of accepted realizations.

(2) Each accepted realization will produce one median value of the studied parameter e.g. median breakthrough time. Variation is defined as the difference between the 90th percentile and the 10th percentile of the distribution of median values as given by the ensemble of accepted realizations.

(3) For each deposition tunnel all paths of all accepted realizations are evaluated as one ensemble of data. The variation is defined as the difference between the 90th percentile and the 10th percentile of these distributions of values (see Table 3-1 and Table 3-2).

As the variation between the realizations is so small at 2,000 AD, and as we define the variation as the difference between the 90th and the 10th percentile, the variation within all flow paths data will be dominated by the variation within the realizations, and it follows that in Table 3-5 there is no difference between the variation within the realizations and the variation for all data when comparing lengths of flow paths at 2,000 AD.

It is a different situation when the breakthrough times are considered, because for the breakthrough time there are considerable variations within and between realizations. For the BLA and the BTF tunnels, the variation within a realization is larger than the variation between realizations. This means that the distribution of flow paths is rather stable when comparing different realizations, but for the BMA, the variation between the realizations is larger than the variation within a realization. For the SILO the variation within and between realizations is approximately the same.

At 5,000 AD, lengths of flow paths and the variation in flow path lengths are larger than at 2,000 AD, but the breakthrough times are shorter at 5,000 AD. The variations in times are smaller as well; this follows from the more complicated flow pattern at 5,000 AD and the increased groundwater flow at 5,000 AD. A comparison of length of flow paths (see Table 3-5). reveals that for BMA, BLA and the SILO, the variation within a realization is larger than the variation between realizations, but the opposite takes place for the BTF tunnels. When comparing breakthrough times we note that the variation within realizations is larger than the variation between realizations for all tunnels except the SILO. For the SILO the variation between realizations is much larger than the variation within the realizations. This follows from the complex spatial distribution of the flow routes from the SILO; the spatial distribution of flow routes from the SILO is significantly different for different values of conductivity of the fracture zones and rock mass (for different realizations). The spatial distribution of the flow routes from the other deposition tunnels are more stable and will not change dramatically between different realizations.

The variations when considering all data are larger than the variations within realizations and also larger than the variation between realizations

It should be noted that the accepted realizations analyzed in this study, i.e. the accepted realizations for which the flow paths were simulated, are the accepted realizations of the base case of the /Holmén 2005/ study. The base case does not include any heterogeneity inside the rock mass or inside the fracture zones; hence the permeability of a unit of the model is represented by a constant value, but the values are different for the different units.

As an alternative case presented in /Holmén 2005/, heterogeneity was also defined within each unit by use of a stochastic continuum approach, but the alternative case is not evaluated in this study. The variation in flow path properties within a realization will be less for the base case than for the alternative case. The variation will be larger for the alternative case as the alternative case also includes heterogeneity within each unit. Therefore we may say that the base case, which is analyzed by use of flow paths in this study, underestimates the variation in flow path properties within a realization.

The reason for focusing this study on the base case of /Holmén 2005/ is that for the alternative case the heterogeneity of the permeability field between identified fractures zones is modelled based on an unconditioned stochastic approach, which may create highly permeable structures (local fractures or fracture zones) between the identified fracture zones and the tunnels, structures that have not been observed in the real tunnels or in the real investigation boreholes. The introduction of a heterogeneous permeability field may create a system of permeable structures that are significantly different from the structural geological interpretation of the actual rock mass at the SFR-repository.

3.4 Example of transport data delivered

As a part of this study a number data sets have been created representing the flow path data for each accepted realization.

For each studied flow situation (2,000 AD and 5,000 AD) and for each one of the 60 accepted realizations there are one set of files. Each set of files consists of 5 different data-files, one data-file for each deposition tunnel. In total 2×60×5 = 600 files.

The data files include statistics for the simulated flow paths for the studied tunnel and also individual values of path length and breakthrough time for 1,000 different flow paths from the deposition tunnel studied.

An example is given on the next page, see Table 3-6. Files of this type have been delivered as part of this study.

It is important to remember that the uncertainty factors (see Chapter 2) are not independent from the flow path data (see Chapter 3). When stochastic calculations are performed by use of a transport model and the data presented in this study is used as input to such calculations, the corresponding uncertainty factors and flow path data should be used. Corresponding data is identified by the number of the row in the matrix of uncertainty factors and the number of the files providing flow path data. Hence, the first row with uncertainty factors should be used together with the flow path data files denoted with number 1, and so on.

Table 3-6. Example of data file defining the flow path data. As discussed in Sections 2.3 and 3.4 the flow paths data should be combined with the corresponding u-factors. The example given below is for realization number 60, it should be combined with the u-factors for realization 60 as given on row 60 of the matrix of u-factors.

FLOW_PATH_DATA

In__data_file..... SEM-5000.DAT
PAT_data_file..... Pares-BMA-60.sto
Res_data_file(in_PAT-file).. Restart file:SEM1_RESN_136k5_Pred5.RES

L1_=_Length_in_tunnel(m)__(in_given_KG)
L2_=_Length_in_rock(m)
L3_=_Total_Length(m)
t2_=_Time_in_rock(a)

Statistics	%	L1(m)	L2(m)	L3(m)	t2(a)
Percentile:	1.0 =	0.000000	72.46284	72.46284	27.13647
Percentile:	5.0 =	0.000000	79.26700	79.26700	35.54668
Percentile:	10.0 =	0.000000	83.41380	83.41380	39.79515
Percentile:	20.0 =	0.000000	88.26860	88.26860	48.45002
Percentile:	30.0 =	0.000000	92.09760	92.09760	55.27460
Percentile:	40.0 =	0.000000	96.12700	96.12700	63.49125
Percentile:	50.0 =	0.000000	100.6700	100.6700	70.14840
Percentile:	60.0 =	0.000000	107.2200	107.2200	78.19824
Percentile:	70.0 =	0.000000	123.1380	123.1380	87.71119
Percentile:	80.0 =	0.000000	131.1540	131.1540	97.51775
Percentile:	90.0 =	0.000000	139.5040	139.5040	109.6994
Percentile:	95.0 =	0.000000	144.0420	144.0420	117.7144
Percentile:	99.0 =	0.000000	150.5688	150.5688	139.9559

---

n	Length_in_rock(m)	Time_in_rock(a)
1	86.64400	36.13965
2	96.98000	35.84475
3	92.84600	38.21030
4	79.27400	37.19241
5	79.00700	37.36048
6	77.63500	33.30796
7	87.73600	34.79515
8	86.04200	38.70815
9	90.86800	36.69774
10	74.79100	30.64783
11	90.72900	33.98973
12	84.08000	37.34145
13	71.47500	26.93588
14	73.34500	28.94850
15	74.27300	26.97330
16	72.67400	26.20465
…		
1055	126.1300	102.8824
1056	115.3300	95.26573

4 Hydraulic importance of tunnel plugs

4.1 Introduction

Before the repository is closed and abandoned low permeable plugs will be installed at different locations in the tunnel system; and all bore holes from the tunnel-system into the surrounding rock masses will be refilled with low permeable concrete. The purpose of these measures is to limit the groundwater flow in the tunnels and to create a physical barrier between the deposition tunnels and the surroundings. In the future it is possible that the tunnel plugs may degrade and no longer be efficient hydraulic barriers. The importance of the tunnel plugs, with respect to the groundwater flow in the tunnels, is discussed in /Holmén and Stigsson 2001a/, Chapter 14. This section is partly based on the results presented in that study, as well as on new simulations.

4.2 Positions of tunnel plugs

The final locations of the tunnel plugs are not decided; for the discussion presented in the following sections we have studied plugs at the following positions, see Figure 4-1.

- In all access tunnels where these tunnels are in contact with the SILO.
- At both ends of the BMA tunnel.
- At both ends of the BLA tunnel.
- At both ends of each BTF tunnel.
- In the two tunnels of the access ramp.

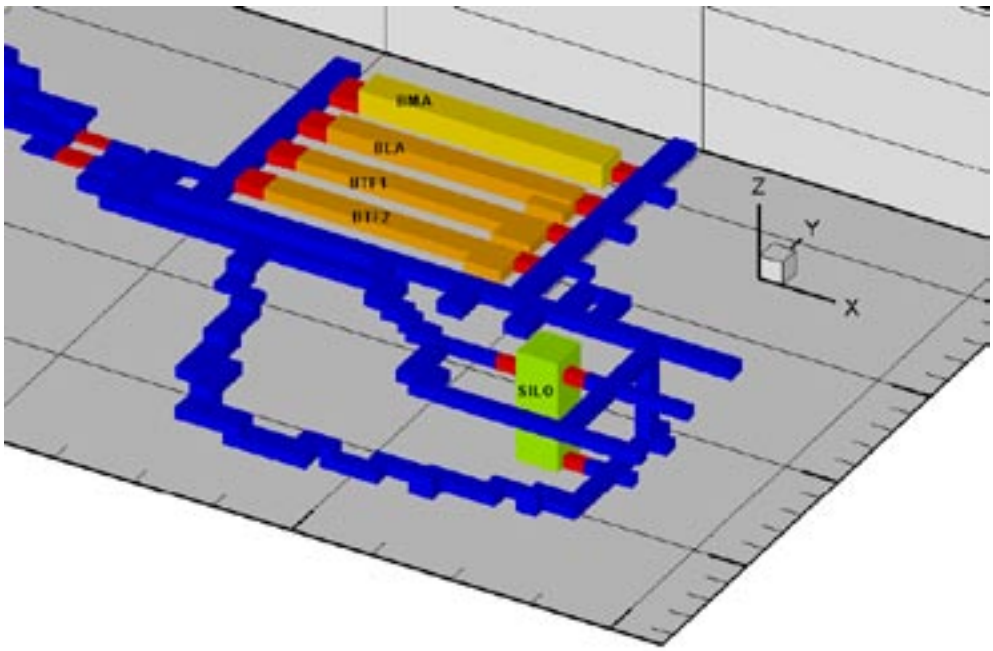

Figure 4-1. *The tunnel system at SFR as implemented in a numerical Geoan model. The positions of the tunnel plugs are given by the red cells.*

4.3 Hydraulic importance of plugs in the access ramp

Above the access ramp there is a topographic ridge, and on this ridge a wave breaker has been constructed. The wave breaker is a part of the SFR harbour. In the future when the sea has retreated from the SFR area, the ridge will be a local topographic surface water divide. The ridge (the wave breaker) above the access-ramp will create a groundwater divide in the access-ramp, also for the situation when the sea covers the repository area, presuming that the ridge/wave breaker is above the sea level. There will be no groundwater flow crossing over the groundwater divide.

A consequence of the groundwater divide in the access ramp is that the plugs in the access ramp are of little importance with regard to the groundwater flow in the ramp. Because, with or without tunnel plugs in the ramp, there will be a groundwater divide in the ramp, and the groundwater flow will be reduced because of the groundwater divide. With or without plugs in the access ramp, the future groundwater flow through the SFR deposition tunnels is close to the same (presuming that the other tunnel plugs are intact). Because of the groundwater divide in the access ramp, the large regional fracture zone intersecting the access ramp (the Singö zone) will not have a large impact on the future flow of the SFR tunnel system.

4.4 Flow pattern in the access tunnels considering flow paths from deposition tunnels

The flow pattern of the flow paths from the deposition tunnels will change if there are no tunnel plugs in the tunnel-system. (The size of the flow in the tunnels will change as well and that is discussed in the next section.)

For the purpose of analysing the hydraulic importance of tunnel plugs and the flow pattern in the access tunnels considering flow paths from the deposition tunnels, we have simulated flow paths from the BLA tunnel and the BTF2 tunnel, for a flow situation with and without tunnel plugs. We have studied two positions of the shore line: 2,000 AD (0 m above sea level) and 4,000 AD (–11 m above sea level). The permeability of the rock mass and the fracture zones were defined in line with the calibrated values given in /Holmén and Stigsson 2001a/.

2,000 AD

As long as the sea covers the SFR repository, the flow pattern of flow paths from the deposition tunnels is generally upwards to the sea-bed. Without tunnel plugs a significant part of the flow paths from the deposition tunnels may move in the access tunnel northeast of the deposition tunnels, before entering the rock mass. This is illustrated in Figure 4-2. The flow paths from the BLA tunnel will however not use the access tunnels at 2,000 AD, with or without the tunnel plugs. The flow paths from the BTF2 tunnels will not move in the access tunnels, if the tunnel plugs are intact. But if there are no plugs, 55% of the paths from the BTF2 tunnel will move in the access tunnel, the median path length for the paths in the access tunnel is calculated to 113 m. Without tunnel plugs, a small amount of the flow paths from the BTF1 and BTf2 tunnel (a few percent) will enter into the other deposition tunnels and use fracture zone 6 for the upward movement to the sea bed.

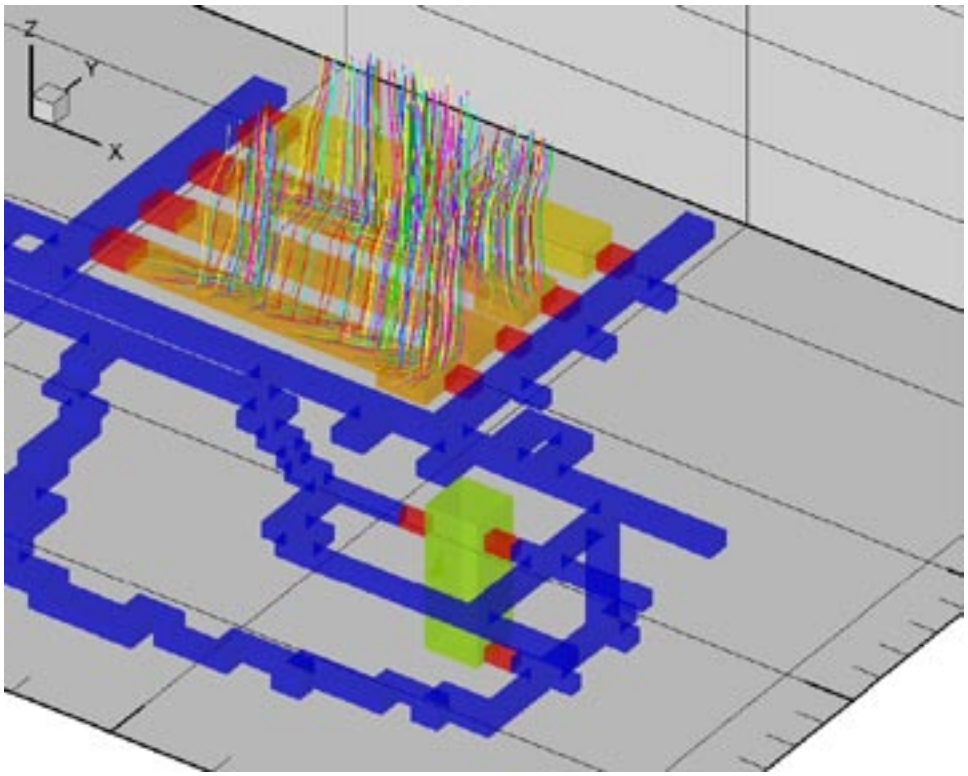

(i) With tunnel plugs.

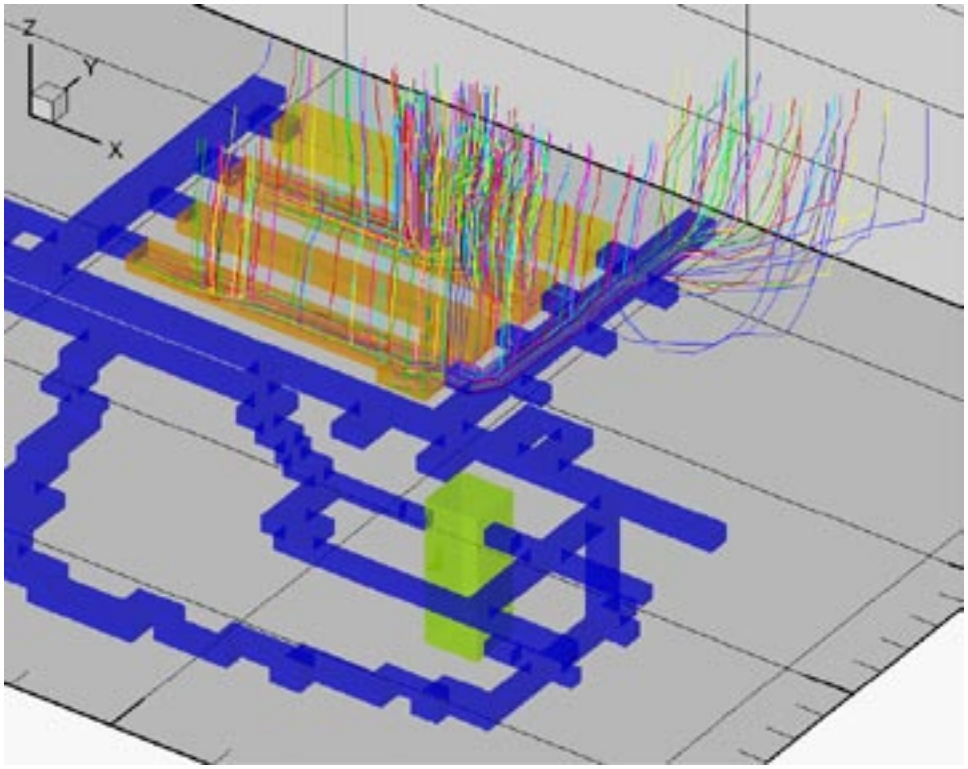

(ii) Without tunnel plugs.

Figure 4-2. *Flow paths from the BLA and BTF2 tunnels considering a repository: (i) with tunnel plugs, and (ii) without tunnel plugs. The flow situation corresponds to 2,000 AD; the sea covers the repository area.*

4,000 AD

Considering a future situation for which the sea has retreated from the repository area, for such a situation the tunnel plugs are very important for the flow pattern. This is illustrated in Figure 4-3, results are also given in Table 4-1 and Table 4-2.

The figures and the tables demonstrate the following. When the tunnel plugs are in place, the flow paths from the deposition tunnels will leave the deposition tunnels and enter the rock mass nearly without any use of the access tunnels, for the BLA 98% will not use the access tunnels and for the BTF2 97% will not use the access tunnels. Without the tunnel plugs a large amount of the flow paths, 40% for BLA and 77% for BTF2, will move in the access tunnels before entering the rock mass. The length of the flow paths inside the access tunnels may be significant, for the BLA the median is 75 m and for the BTF2 the median is 193 m.

Table 4-1. Length and breakthrough time of low paths in access tunnels, with and without tunnel plugs. Flow paths from the BLA tunnel. The flow situation corresponds to 4,000 AD; the sea has retreated form the repository area and is at an elevation of –11 m above sea level.

BLA 4,000AD (1)	With tunnel plugs	No tunnel plugs (2)
Amount of paths using the access tunnels	2%	40%
Length of paths in access tunnels	*Percentiles for paths in access tunnels*	*Percentiles for paths in access tunnels*
	10^{th} = 1 m	10^{th} = 14 m
	50^{th} = 6 m	50^{th} = 75 m
	90^{th} = 41 m	90^{th} = 96 m
Advective breakthrough time in access tunnels	*Percentiles for paths in access tunnels*	*Percentiles for paths in access tunnels*
	10^{th} = 15 years	10^{th} = 4 years
	50^{th} = 200 years	50^{th} = 19 years
	90^{th} = 600 years	90^{th} = 36 years

(1) Properties of rock mass and zones are in line with the calibrated case of /Holmén and Stigsson 2001a/.
(2) Access tunnels with back-fill: K=1E–6 m/s, Effective porosity=10%

Table 4-2. Length and breakthrough time of low paths in access tunnels, with and without tunnel plugs. Flow paths from the BTF2 tunnel. The flow situation corresponds to 4,000 AD; the sea has retreated form the repository area and is at an elevation of –11 m.a.s.l.

BTF2 4,000AD (1)	With tunnel plugs	No tunnel plugs (2)
Amount of paths using the access tunnels	7%	77%
Length of paths in access tunnels	*Percentiles for paths in access tunnels*	*Percentiles for paths in access tunnels*
	10^{th} = 5 m	10^{th} = 38 m
	50^{th} = 125 m	50^{th} = 193 m
	90^{th} = 165 m	90^{th} = 214 m
Advective breakthrough time in access tunnels	*Percentiles for paths in access tunnels*	*Percentiles for paths in access tunnels*
	10^{th} = 13 years	10^{th} = 10 years
	50^{th} = 32 years	50^{th} = 20 years
	90^{th} = 210 years	90^{th} = 41 years

(1) Properties of rock mass and zones are in line with the calibrated case of /Holmén and Stigsson 2001a/.
(2) Access tunnels with back-fill: K=1E–6 m/s, Effective porosity=10%

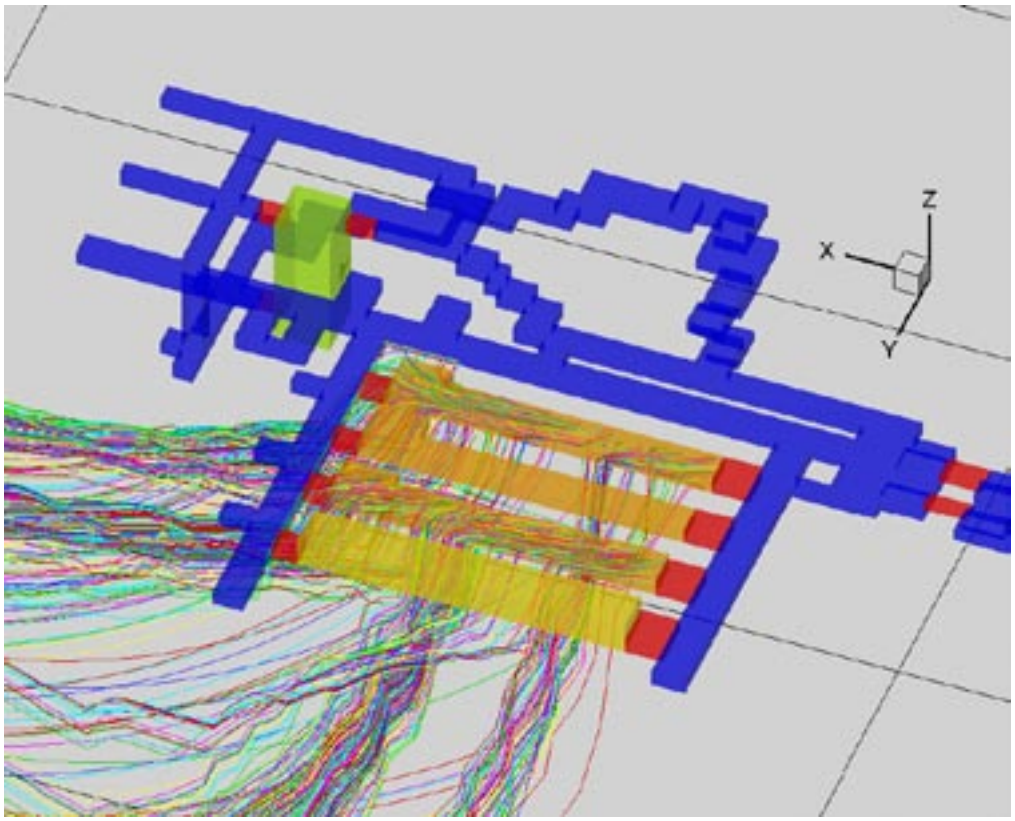

(i) With tunnel plugs.

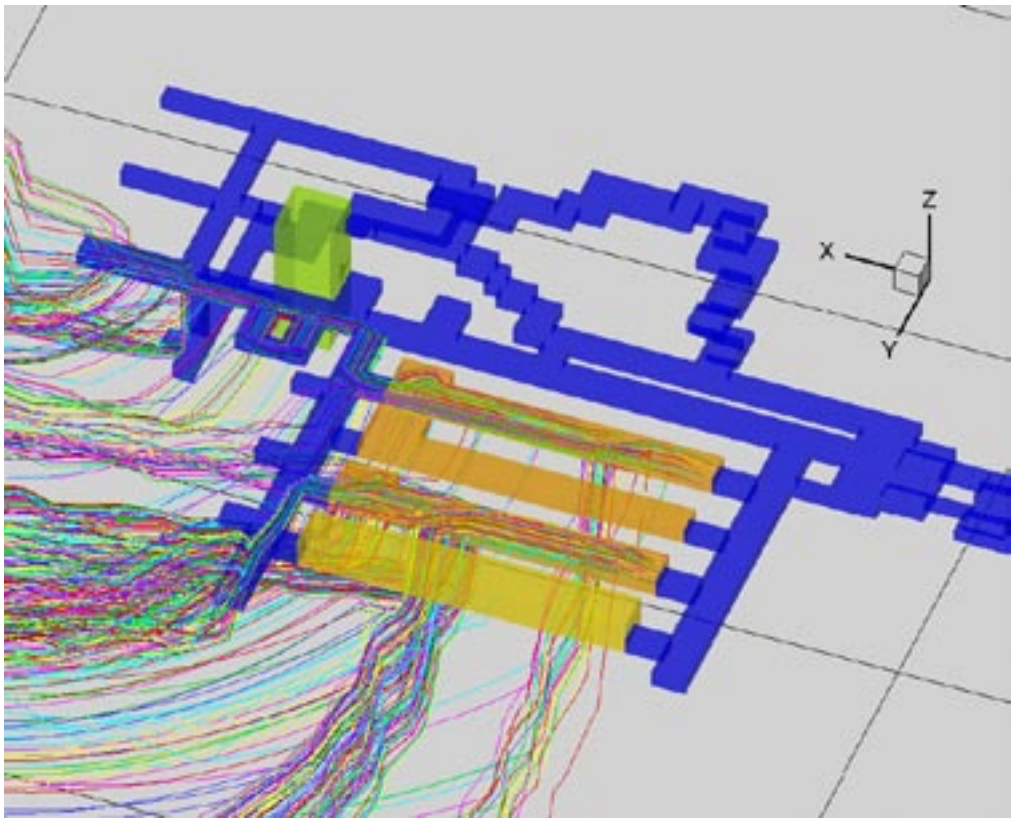

(ii) Without tunnel plugs.

Figure 4-3. *Flow paths from the BLA and BTF2 tunnels considering a repository: (i) with tunnel plugs, and (ii) without tunnel plugs. The flow situation corresponds to 4,000 AD, the sea has retreated form the repository area, the elevation of the sea is –11 m above sea level.*

4.5 Flow in deposition tunnels with fully degraded plugs

The flow values given below are taken from /Holmén and Stigsson 2001a/, Chapter 14.

The calculation of total flow is based on a mass balance taken over the envelope of the studied structure. The total flow provides no information of the length of the flow paths in the tunnels, a short path or a long path, will both add to the total flow.

Considering the detailed model of /Holmén and Stigsson 2001ab/, and a situation without tunnel plugs, the total flow (m^3/year) in the tunnels will change as follows:

BMA:

- At 2,000 AD an increase in flow with a factor of 1.1 in the waste domain and an increase in flow with a factor of 1.4 considering the whole tunnel.
- At 4,000 AD an increase in flow with a factor of 2.3 in the waste domain and an increase in flow with a factor of 2.5 considering the whole tunnel.

BLA:

- At 2,000 AD an increase in flow with a factor of 1.1 in the waste domain and an increase in flow with a factor of 1.2 considering the whole tunnel.
- At 4,000 AD an increase in flow with a factor of 1.5 in the waste domain and an increase in flow with a factor of 1.6 considering the whole tunnel.

BTF1:

- At 2,000 AD a decrease in flow with a factor of 0.87 in the waste domain and an increase in flow with a factor of 1.4 considering the whole tunnel.
- At 4,000 AD a decrease in flow with a factor of 0.70 in the waste domain and an increase in flow with a factor of 1.2 considering the whole tunnel.

BTF2:

- At 2,000 AD a decrease in flow with a factor of 0.87 in the waste domain and an increase in flow with a factor of 1.4 considering the whole tunnel.
- At 4,000 AD a decrease in flow with a factor of 0.80 in the waste domain and an increase in flow with a factor of 1.6 considering the whole tunnel.

SILO:

- At 2,000 AD a decrease in flow with a factor of 0.70 in the waste domain (i.e. the concrete SILO) and an increase in flow with a factor of 14.5 considering the open volume above the concrete SILO.
- At 4,000 AD an increase in flow with a factor of 1.56 in the waste domain (i.e. the concrete SILO) and an increase in flow with a factor of 26.4 considering the open volume above the concrete SILO.

For some of the deposition tunnels (e.g. BTF1) the total flow of the whole tunnel will increase, but the total flow of the waste domain will decrease for a situation without tunnel plugs. This follows from the changed direction of the flow in the tunnels and especially in the waste domains. This is discussed in more detail /Holmén and Stigsson 2001ab/.

5 Conclusions

The purposes of this study are to calculate and to deliver to SKB two different sets of data: (i) uncertainty factors and (ii) flow path data.

Uncertainty factors are produced for two different flow situations, corresponding to 2,000 AD (the sea covers the repository) and 4,000 AD (the sea has retreated form the repository area). Uncertainty factors are produced for the different deposition tunnels, considering the base case of /Holmén 2005/ and the 60 realisation that passed all tests of the inverse modelling procedure presented in /Holmén 2005/. The uncertainty factors are discussed in Chapter 2 and two lists (matrix) of uncertainty factors have been delivered as a part of this study.

Flow paths are produced for two different flow situations, corresponding to 2,000 AD (the sea covers the repository) and 5,000 AD (the sea has retreated form the repository area). Flow paths from the different deposition tunnels have been simulated, considering the above discussed base case and the 60 realisation that passed all tests of this base case. The flow paths are presented and discussed in Chapter 3 and files presenting the results of the flow path analyses have been delivered as part of this study.

The uncertainty factors (see Chapter 2) are not independent from the flow path data (see Chapter 3). When stochastic calculations are performed by use of a transport model and the data presented in this study is used as input to such calculations, the corresponding uncertainty factors and flow path data should be used. Corresponding data is identified by the number of the row in the matrix of uncertainty factors and the number of the files providing flow path data. Hence, the first row with uncertainty factors should be used together with the flow path data files denoted with number 1, and so on.

This study also includes a brief discussion of the hydraulic importance of tunnel plugs (see Chapter 4).

6 References

Holmén J G, 1992. A three-dimensional finite difference model for calculation of flow in the saturated zone. Department of quaternary geology, Uppsala University, Uppsala, Sweden, ISBN 91-7376-119-2, ISSN 0348-2979.

Holmén J G, 1997. On the flow of groundwater in closed tunnels. Generic hydrogeological modelling of nuclear waste repository, SFL 3-5. SKB TR 97-10,
Svensk Kärnbränslehantering AB.

Holmén J G, Stigsson M, 2001a. Modelling of Future Hydrogeological Conditions at SFR, Forsmark. SKB R-01-02, Svensk Kärnbränslehantering AB.

Holmén J G, Stigsson M, 2001b. Details of predicted flow in deposition tunnels at SFR, Forsmark. SKB R-01-21, Svensk Kärnbränslehantering AB.

Holmén, 2005. SFR-1. Inverse modelling of inflow to tunnels and propagation of estimated uncertainties to predictive stages. SKB R-05-74, Svensk Kärnbränslehantering AB.

SSI 2003:21, SKI 2003:37. Dverstorp B. and Sundström B et.al. SSI:s och SKI:s granskning av SKB:s uppdaterade Slutlig Säkerhetsrapport för SFR I. Granskningsrapport. Statens strål-skyddsinstitut och Statens kärnkraftsinspektion. Oktober 2003. SSI. Statens Strålskyddsinstitut; SE-17116 Stockholm, Sweden.

Pollock D W, 1989. Documentation of computer program to compute and display path lines using results from the U.S. Geological survey modular three-dimensional finite difference groundwater flow model, (Modpath manual). US Geological survey, 411 National Centre Reston, VA 22092, USA.

Appendix A

Visualisation of tunnels and fracture zones

A brief visualization of the tunnels and fracture zones as included in the semi-regional model is presented below. The tunnels are included in the calculation grid as explicit structures. The zones are included in the calculation grid by use of an implicit formulation; hence the angular shape (zigzag shape) of the zones is given by the shape of the cells of the finite difference grid.

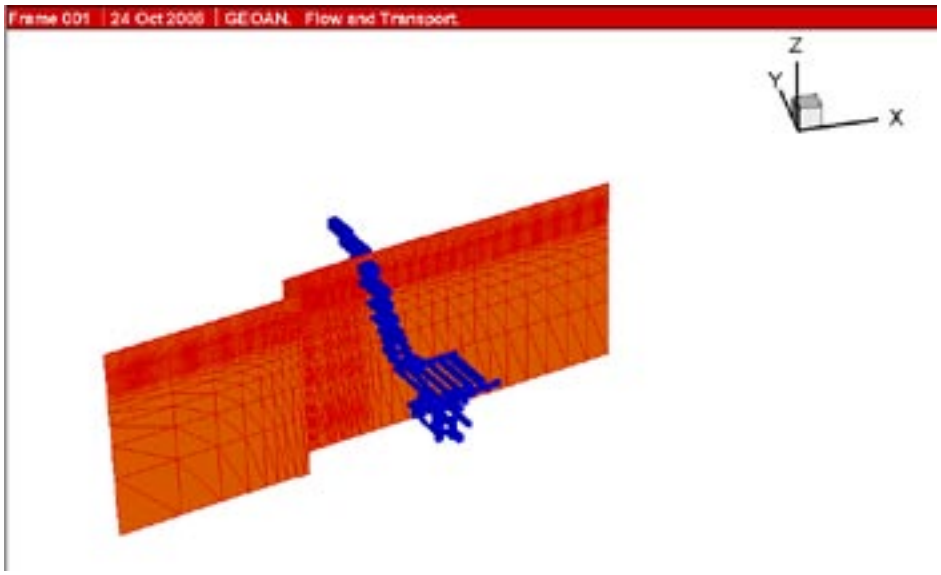

The tunnels (blue) and the Singö fracture zone (orange).

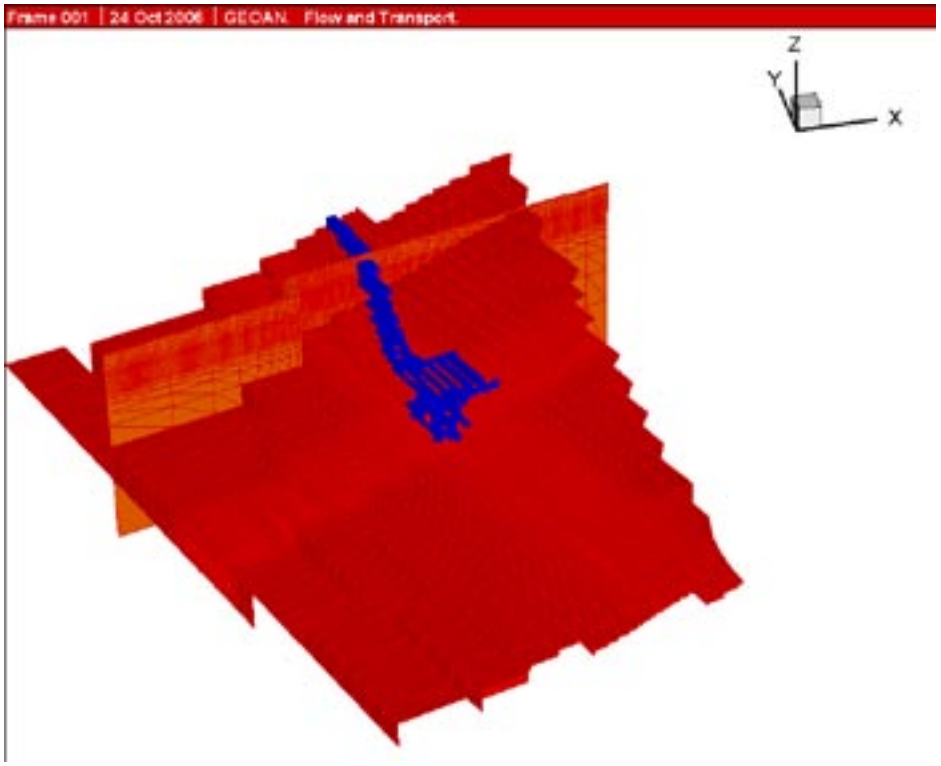

The tunnels, the Singö fracture zone and the sub-horizontal zone H2 (red).

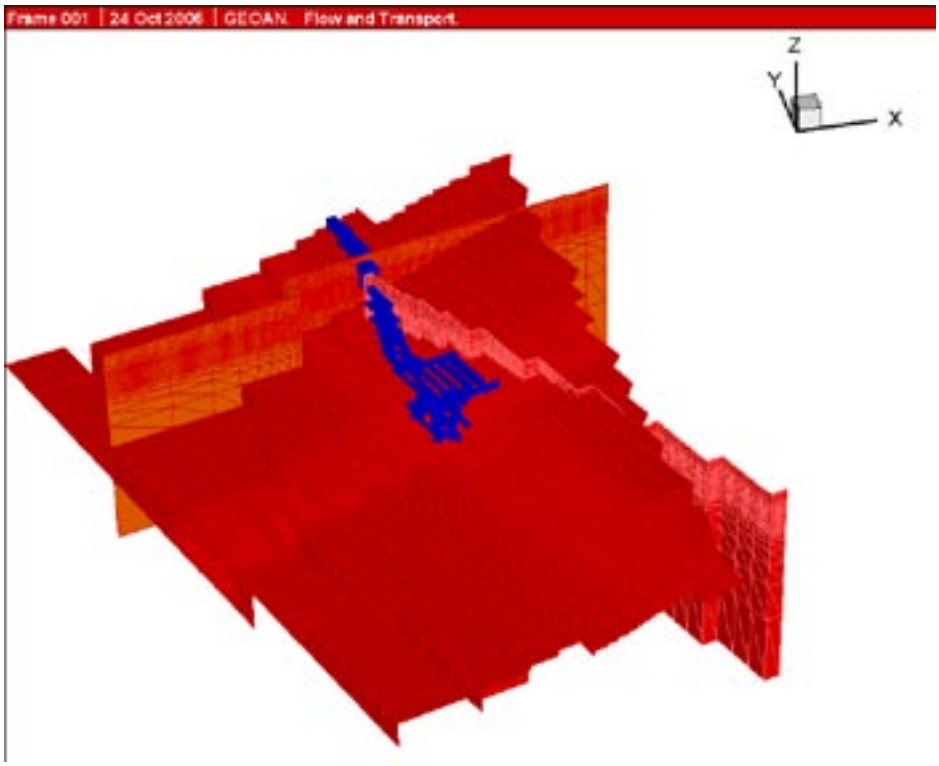

The tunnels, the Singö fracture zone, the sub-horizontal zone H2 and the sub-vertical zone 3.

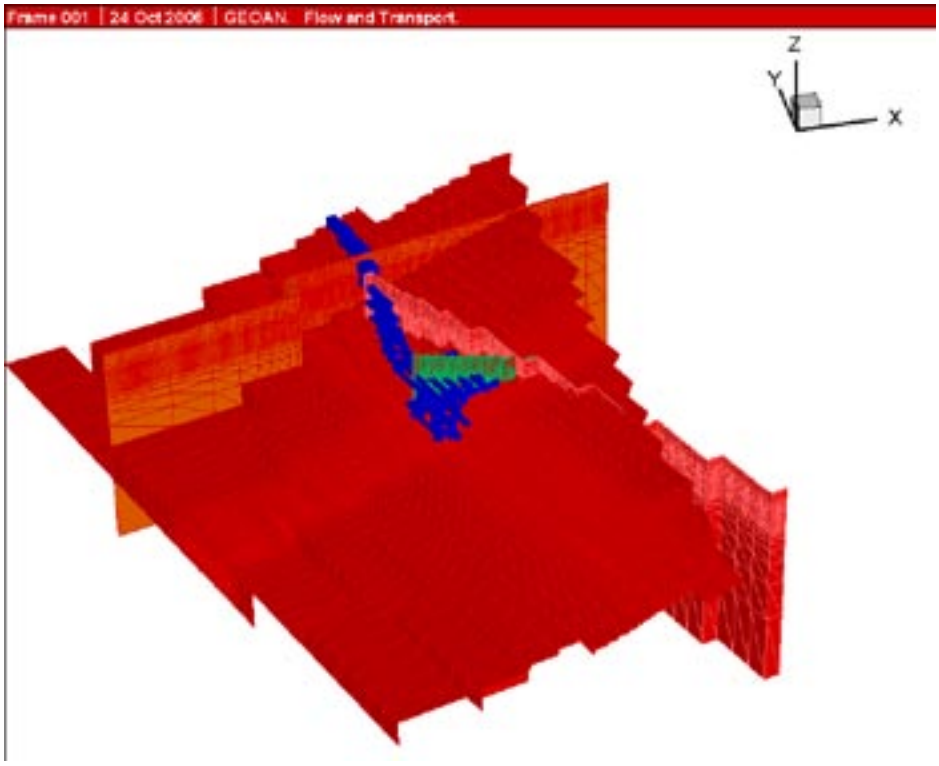

The tunnels, the Singö fracture zone, the sub-horizontal zone H2 and Zone 3, as well as Zone 6 (green).

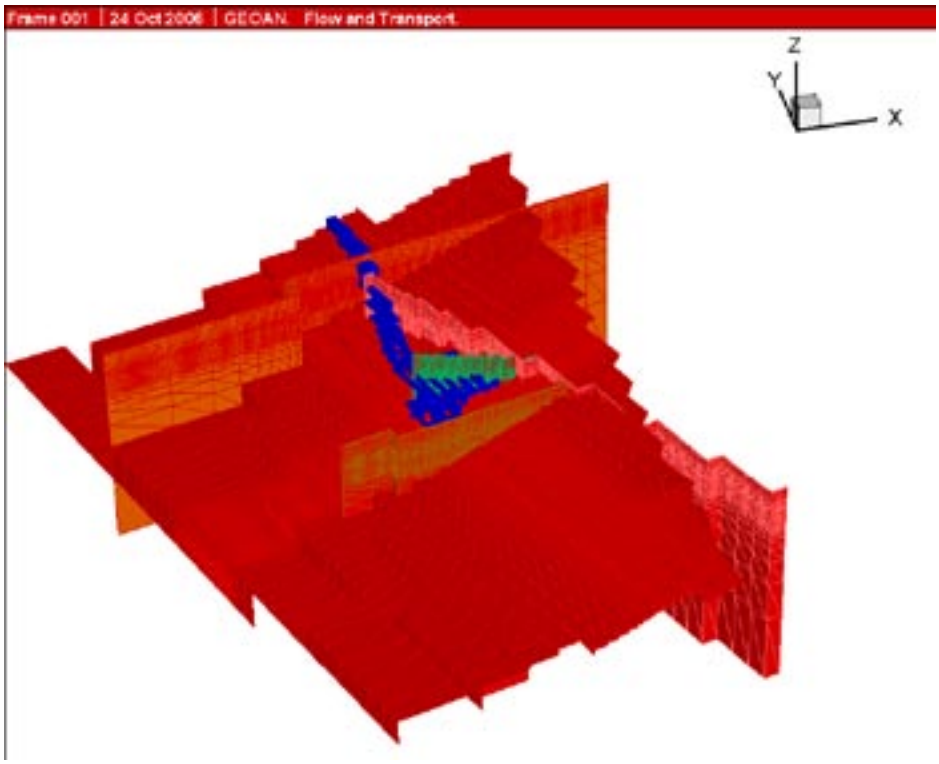

The tunnels, the Singö fracture zone, the sub-horizontal zone H2, Zone 3 and Zone 6 (green) as well as Zone 8 (brown).

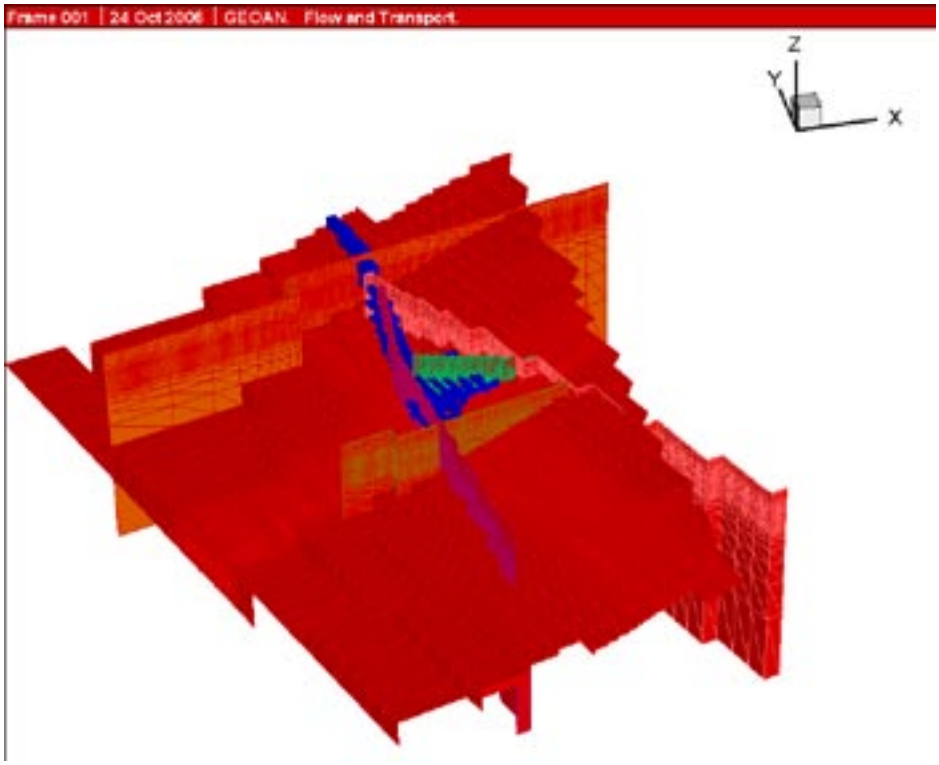

The tunnels, the Singö fracture zone, the sub-horizontal zone H2, Zone 3, Zone 6 (green) and Zone 8 (brown) as well as Zone 9 (purple).